(2)

TECHNICAL REPORT BRL-TR-3093

BRL

A COMPARISON BETWEEN EXPERIMENT AND SIMULATION FOR CONCEPT VIC REGENERATIVE LIQUID PROPELLANT GUNS, II. 105 MM

TERENCE P. COFFEE
GLORIA P. WREN
WALTER F. MORRISON

APRIL 1990

U.S. ARMY LABORATORY COMMAND

BALLISTIC RESEARCH LABORATORY
ABERDEEN PROVING GROUND, MARYLAND

NOTICES

Destroy this report when it is no longer needed. DO NOT return it to the originator.

Additional copies of this report may be obtained from the National Technical Information Service, U.S. Department of Commerce, 5285 Port Royal Road, Springfield, VA 22161.

The findings of this report are not to be construed as an official Department of the Army position, unless so designated by other authorized documents.

The use of trade names or manufacturers' names in this report does not constitute indorsement of any commercial product.

REPORT DOCUMENTATION PAGE

Form Approved
OMB No. 0704-0188

1. AGENCY USE ONLY (Leave blank)	2. REPORT DATE	3. REPORT TYPE AND DATES COVERED
	April 1990	Final

4. TITLE AND SUBTITLE
A Comparison Between Experiment and Simulation for Concept VIC Regenerative Liquid Propellant Guns, II. 105 MM

5. FUNDING NUMBERS
PR: 1L263004D155
WU: DA30 6711

6. AUTHOR(S)
Terence P. Coffee, Gloria P. Wren, Walter F. Morrison

7. PERFORMING ORGANIZATION NAME(S) AND ADDRESS(ES)

8. PERFORMING ORGANIZATION REPORT NUMBER

9. SPONSORING / MONITORING AGENCY NAME(S) AND ADDRESS(ES)
US Army Ballistic Research Laboratory
ATTN: SLCBR-DD-T
Aberdeen Proving Ground, MD 21005-5066

10. SPONSORING / MONITORING AGENCY REPORT NUMBER
BRL-TR-3093

11. SUPPLEMENTARY NOTES
The authors are indebted to Lou Ann Walter, Inder Magoon, Minh Luu, and Al Maynard of the General Electric Corporation for their help in providing data and understanding the gun operation.

12a. DISTRIBUTION / AVAILABILITY STATEMENT
Approved for public release; distribution unlimited.

12b. DISTRIBUTION CODE

13. ABSTRACT (Maximum 200 words)
Regenerative liquid propellant gun (RLPG) technology is sufficiently mature to allow the testing of the first 155 mm liquid propellant gun. In support of the development of this artillery weapon, test fixtures in 30 mm and 105 mm sizes have been built and fired. This report describes the analysis and modeling of the 105 mm gun fixture. A previous report discussed the 30 mm gun fixture, and a future report will concentrate on the 155 mm gun. The model is first benchmarked against a series of long charge firings. The process of choosing input values for the gun code is discussed in detail. The model is then used to predict the performance of a medium charge firing and a short charge firing. Finally, further analysis of the data is presented in which assumptions governing the selection of values for the empirical parameters are modified.

14. SUBJECT TERMS	15. NUMBER OF PAGES
Liquid Monopropellant; Concept VIC; Regenerative Gun; Lumped Parameter Model	84
	16. PRICE CODE

17. SECURITY CLASSIFICATION OF REPORT	18. SECURITY CLASSIFICATION OF THIS PAGE	19. SECURITY CLASSIFICATION OF ABSTRACT	20. LIMITATION OF ABSTRACT
UNCLASSIFIED	UNCLASSIFIED	UNCLASSIFIED	UL

INTENTIONALLY LEFT BLANK.

TABLE OF CONTENTS

INTENTIONALLY LEFT BLANK.

LIST OF FIGURES

INTENTIONALLY LEFT BLANK.

LIST OF TABLES

INTENTIONALLY LEFT BLANK.

ACKNOWLEDGMENT

The authors are indebted to Lou Ann Walter, Inder Magoon, Minh Luu, and Al Maynard of the General Electric Corporation for their help in providing data and understanding the gun operation.

INTENTIONALLY LEFT BLANK.

1. INTRODUCTION

Regenerative liquid propellant gun (RLPG) technology is sufficiently mature to allow the testing of the first 155 mm liquid propellant gun. In support of the development of this artillery weapon, test fixtures in 30 mm and 105 mm sizes have been built and fired. The data from all three of these fixtures have been extensively analyzed to better understand the regenerative liquid propellant gun (RLPG) process. This paper reviews the 105 mm data for the Concept VIC configuration, the design chosen for the 155 mm gun, and examines the modeling of that data. A previous paper discussed the 30 mm gun fixture, and a subsequent paper will focus on the 155 mm data.

The structure for the modeling effort discussed in this paper is dictated by the proposed transition of the liquid propellant (LP) program from the Ballistic Research Laboratory (BRL) to the Army Research, Development and Engineering Center (ARDEC). The transition criteria specify that it should be possible to demonstrate agreement between model and test data for 30 mm, 105 mm, and 155 mm by matching mean, filtered pressure-time to within 5% in pressure for damper, reservoir, chamber, and bore and by matching muzzle velocity to within 2%.[1] In addition, it was desired to extend the modeling exercise by attempting to predict performance of different charge sizes based on a calibration of model parameters.

This report documents the modeling of the 105 mm Concept VIC data. First, a description of the Concept VIC fixture is given. The gun code utilized has been described in previous publications.[2,3] The modeling modifications pertinent to the Concept VIC design were described in detail in the first paper of this series which documented the 30 mm Concept VIC gun.[4] The choice of input parameters for the 105 mm is described, most of which are determined from the physical characteristics of the gun. However, some parameters cannot be determined directly and are chosen based on empirical evidence. A series of shots, referred to as the repeatability series, is used to meet the transition criteria and calibrate the code. Once the baseline parameters have been chosen, these values are used to predict the performance of different charge sizes. In general, the predictions are reasonable. A discussion of the data under varying assumptions about the injection and breakup of the liquid propellant, a poorly understood portion of the process, is also included.

2. THE CONCEPT VIC LIQUID PROPELLANT GUN

A generic VIC liquid propellant gun is shown in Figures 1-3. The monopropellant in the liquid reservoir is between the control piston (or control rod) and the outer injection piston. A primer is ignited and injects hot gas into the combustion chamber. As the combustion chamber is pressurized, the control piston is pushed to the rear, opening an injection vent. The outer piston will follow the control piston, injecting the propellant into the combustion chamber.

The motion of the control rod is controlled by the damper assembly. After the initial seal between the control piston and injection piston is broken, the liquid pressure has very little effect on the rod. As the control rod moves, damper fluid is forced through the damper orifice. Three flat areas are machined on the damper rod to control the vent area.

The injection piston will follow the control rod in response to the differential pressure in the liquid reservoir and the combustion chamber. As the injection piston moves close to the control piston, the vent area will decrease, the liquid pressure will increase, and the injection piston will slow down. As the injection piston moves further from the control piston, the vent area will increase, the liquid pressure will decrease, and the injection piston will accelerate.

At the beginning of the stroke, the damper is designed to keep the pistons moving slowly. If the pistons move too rapidly, too much liquid may be injected early and may quench the combustion process. Near the end of stroke, the damper vent area becomes small, bringing the control rod to a gradual halt.

The fixture utilized in the firings discussed in this report was provided under contract by the General Electric Corp (GE). The fixture description and test results have been previously presented.[5]

3. BASIC ASSUMPTIONS

The basic physical assumptions of the model and changes in the governing equations necessary to model a VIC gun fixture were discussed in the first paper in the series.[4]

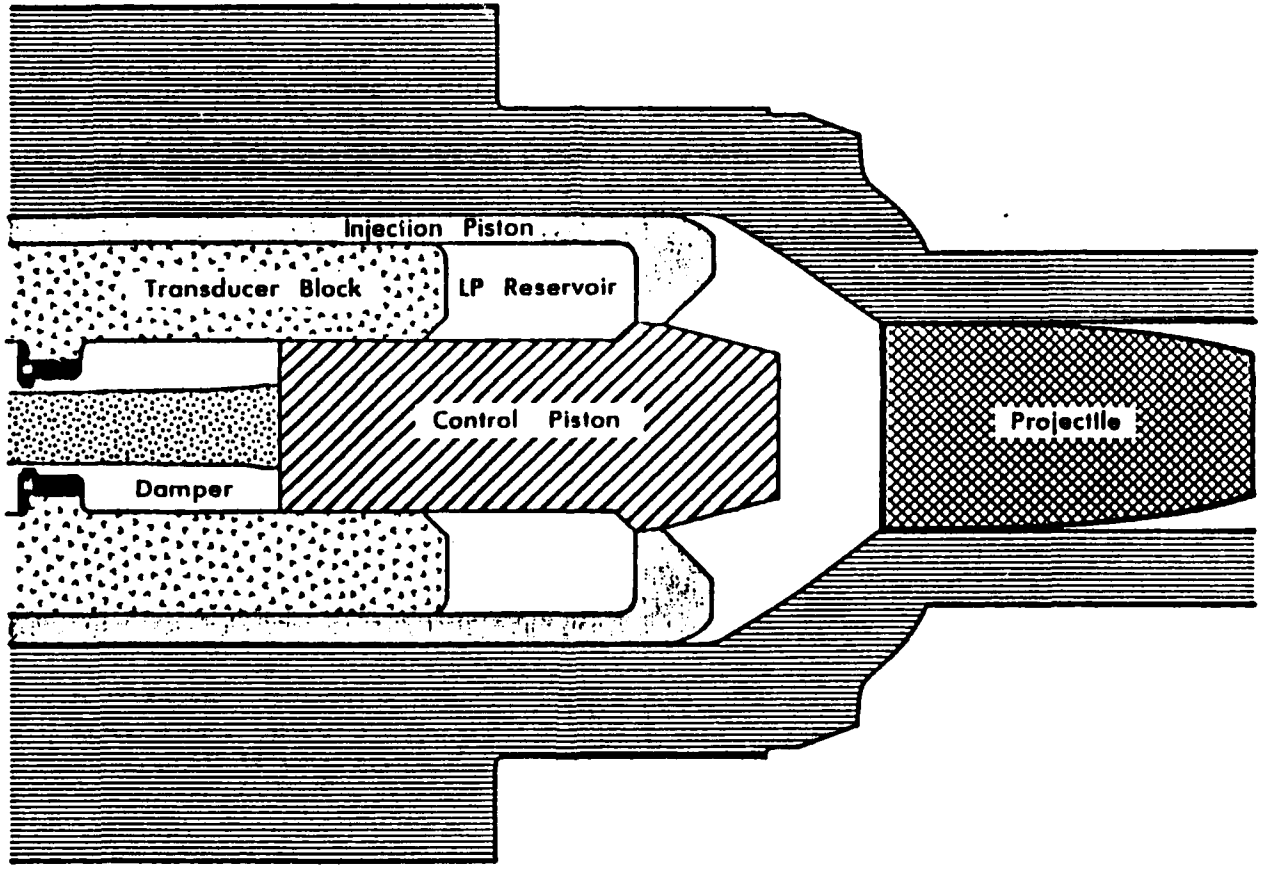

Figure 1. A Concept VIC Regenerative Liquid Propellant Gun, Initial Position.

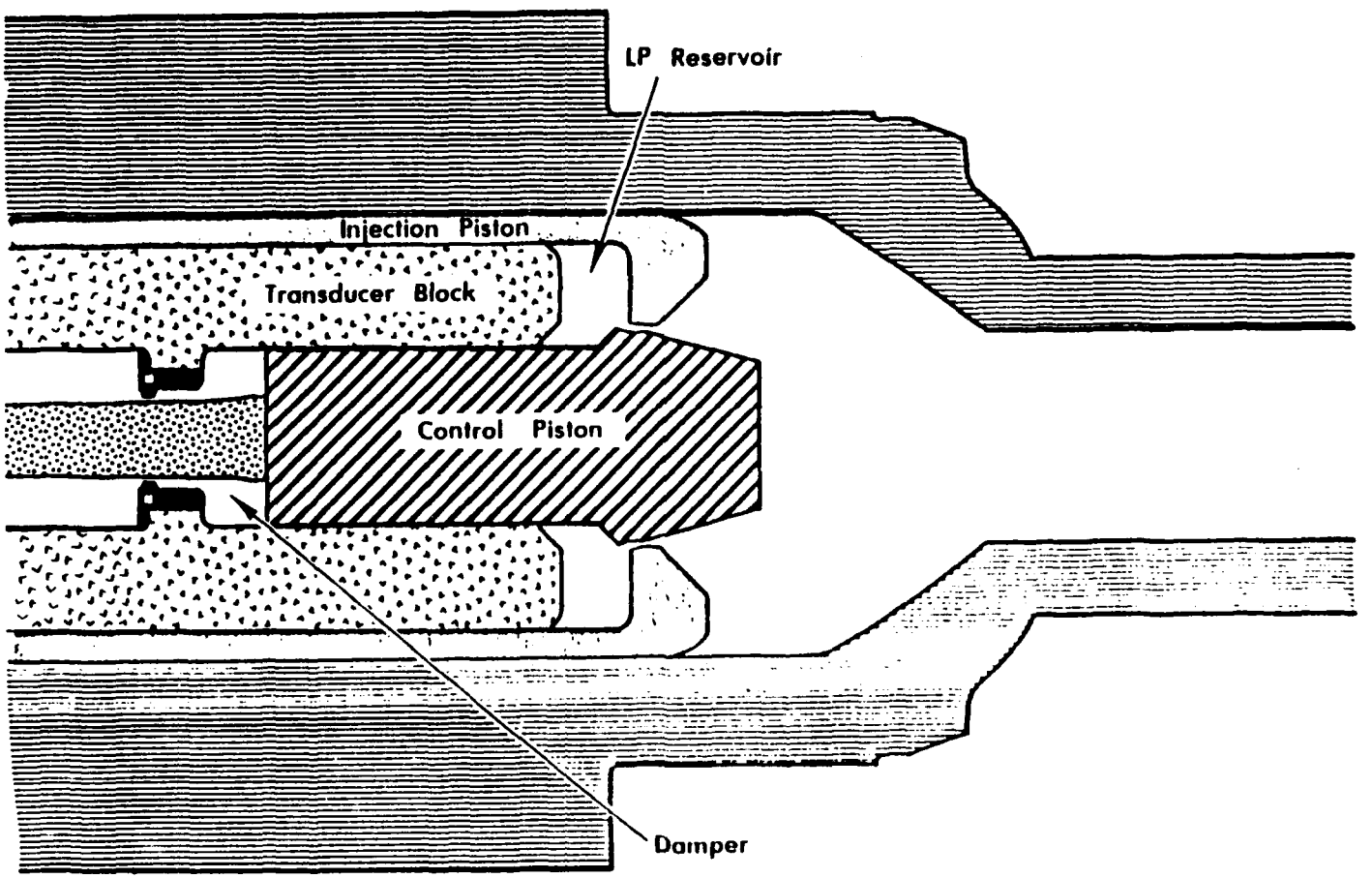

Figure 2. A Concept VIC Regenerative Liquid Propellant Gun, Middle of Stroke.

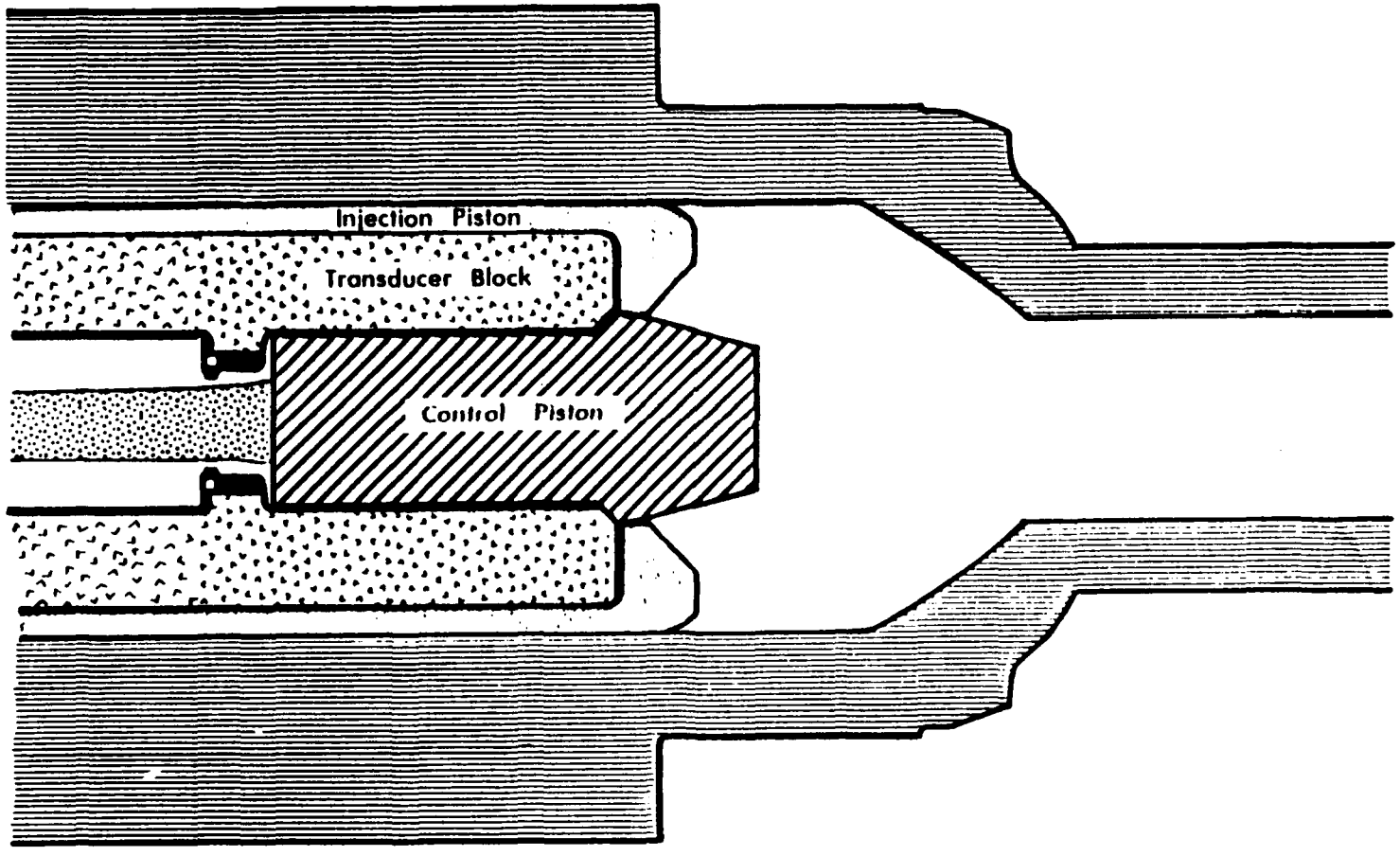

Figure 3. A Concept VIC Regenerative Liquid Propellant Gun, End of Stroke.

4. 105 MM CONCEPT VIC DATA

The 105 mm Concept VIC RLPG was tested using LGP1846 to evaluate the gun design's performance using different charge lengths and initial chamber volumes in preparation for implementing the concept in a 155 mm RLPG.[6] Table 1 shows the primary test parameters used. Besides these differences, the damper region was modified during the short and medium charge firings to improve the ballistic cycle at the end of the piston stroke. Also, the damper fluid was changed from water to Brayco 783 at shot 6. For the long charge firings, the hardware was unchanged. This last set of shots is referred to as the repeatability series.

TABLE 1. 105 mm Concept VIC Test Parameters.

Charge	Short	Medium	Long
Shots	1-7	8-16	17-26
Propellant Volume (cc)	656	1312	1969
Initial Chamber Volume (cc)	3409	2278	1901
Projectile Weight (kg)	19.6	19.6	17.5
Total Igniter Charge (kg)	0.1685	0.1685	0.1685

5. GE 105 MM GUN FIXTURE - BASELINE

The best characterized 105 mm Concept VIC experiments are the long charge repeatability tests (shots 17-26). The mean muzzle velocity for this series of tests is 666.4 m/s with a standard deviation of 0.35%. Although the muzzle velocity repeatability is good, the pressure measurements show some discrepancies, particularly at maximum pressure and after.

The combustion chamber pressure for two shots at two gauge locations is shown in Figure 4. The gauge locations are in the same plane near the front of the combustion chamber (near the initial position of the pistons), and the pressures should be nearly the same, particularly since the muzzle velocity for the two shots is almost identical. The startup and rise to maximum pressure are nearly identical. However, the gauge measurements begin to diverge at maximum pressure with noticeable differences in the expansion regime. A careful consideration of Figure 4 shows that each shot, in this case shots 18 and 26, has one gauge which records high (H120) and one gauge which reads low (H270) with differences of up to 6%. The differences for the recorded pressures at H120 and H270 are probably due to different amounts of drift due to thermal heating.

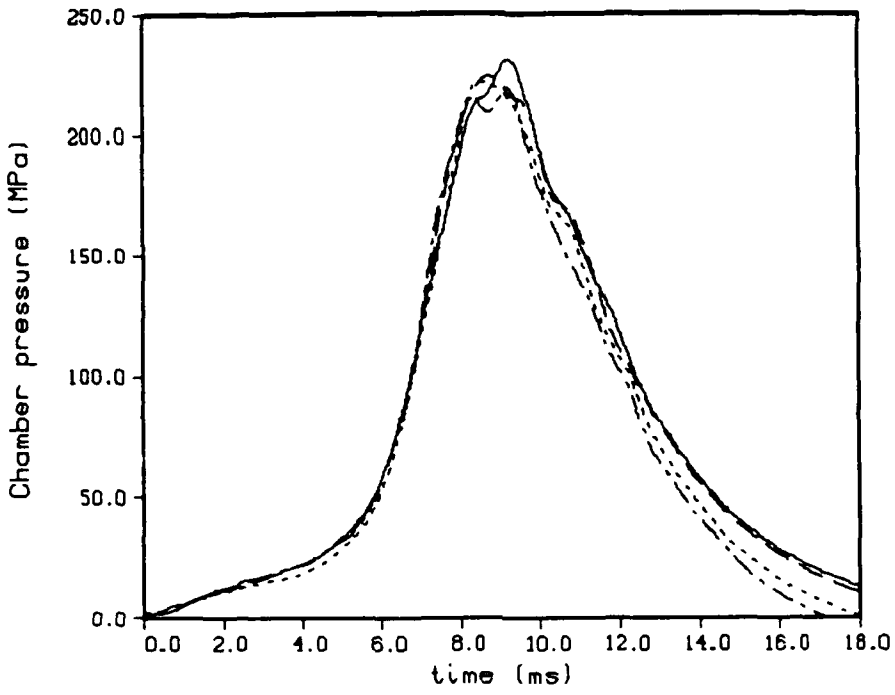

Figure 4. Experimental Chamber Pressure. Round 26 - Gauge H120 (line) and Gauge H270 (dot). Round 18 - Gauge H120 (dash) and Gauge H270 (dot-dash).

The pressure gauge H270 is located opposite to the igniter vent and is exposed to hot gases for a longer time period. Thus H270 shows more drift at the end of the ballistic cycle.

A similar comparison for the liquid pressure for the same two shots from gauges in the same plane mounted in the transducer block is shown in Figure 5. The agreement in maximum pressure is much better than for the 30 mm gun firings.[4] The variation at maximum pressure and after is up to 3%. Figure 6 compares the damper pressures for the two shots. There is only one gauge in the damper area, and the agreement is much better than for the liquid and chamber pressures. Figure 7 shows the total travel (consists of piston motion plus gun recoil) for the control piston and the injection piston, and the recorded travels agree. Since the recoil has not been measured for this gun, a simple free recoil model is used. The primary unbalanced pressure in the system is the combustion chamber pressure. Before shot start, recoil is assumed to be negligible. After shot start, a force equal to the chamber pressure times the gun tube area acts on the fixture. This is integrated numerically to obtain the gun recoil. When this calculated recoil is subtracted from the experimental piston travel, the results, shown in Figure 8, show that the piston travel now levels off at the end of stroke at almost exactly the measured stroke length.

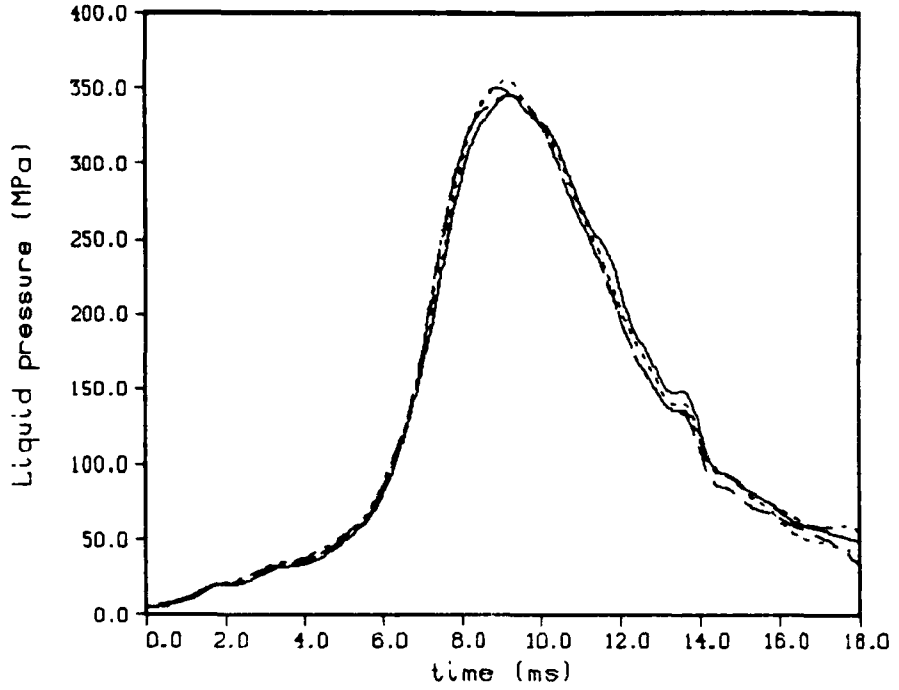

Figure 5. Experimental Liquid Pressure. Round 26 - Gauge LP120 (line) and Gauge LP240 (dot). Round 18 - Gauge LP120 (dash) and Gauge LP240 (dot-dash).

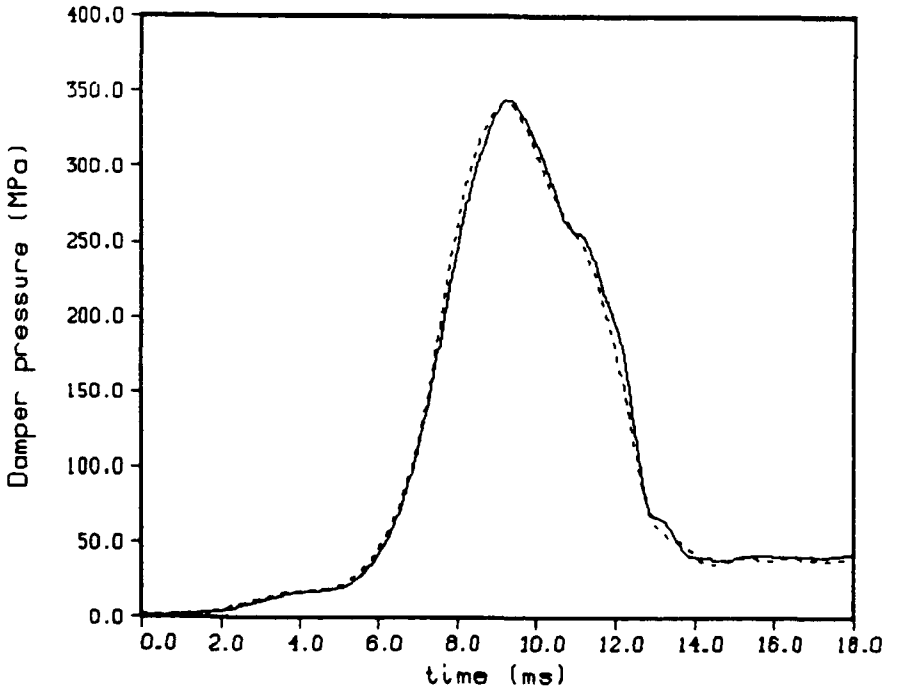

Figure 6. Experimental Damper Pressure. Round 26 (line). Round 18 (dot).

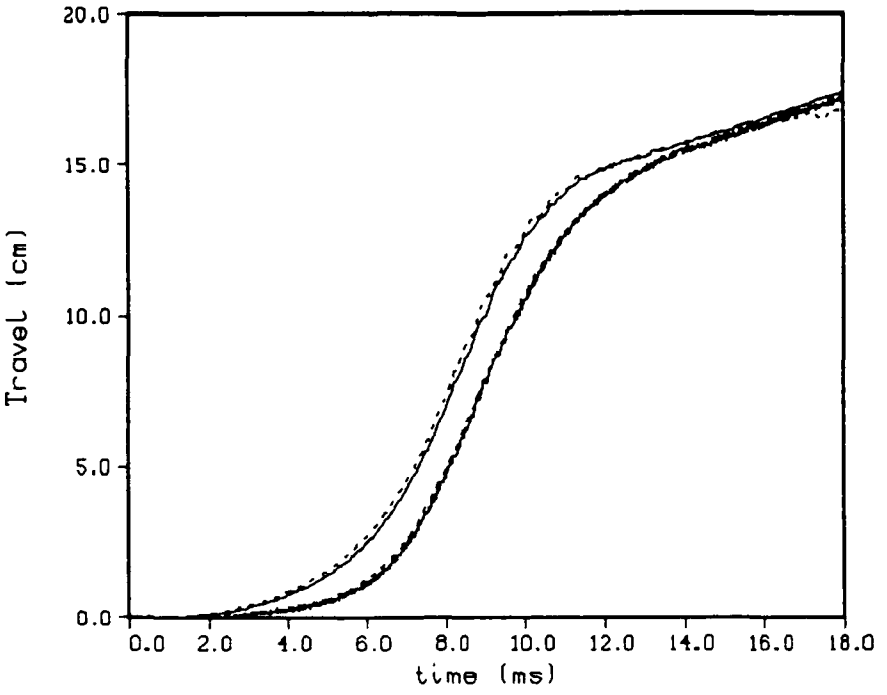

Figure 7. Experimental Piston Travels Including Recoil. Round 26 (line). Round 18 (dot).

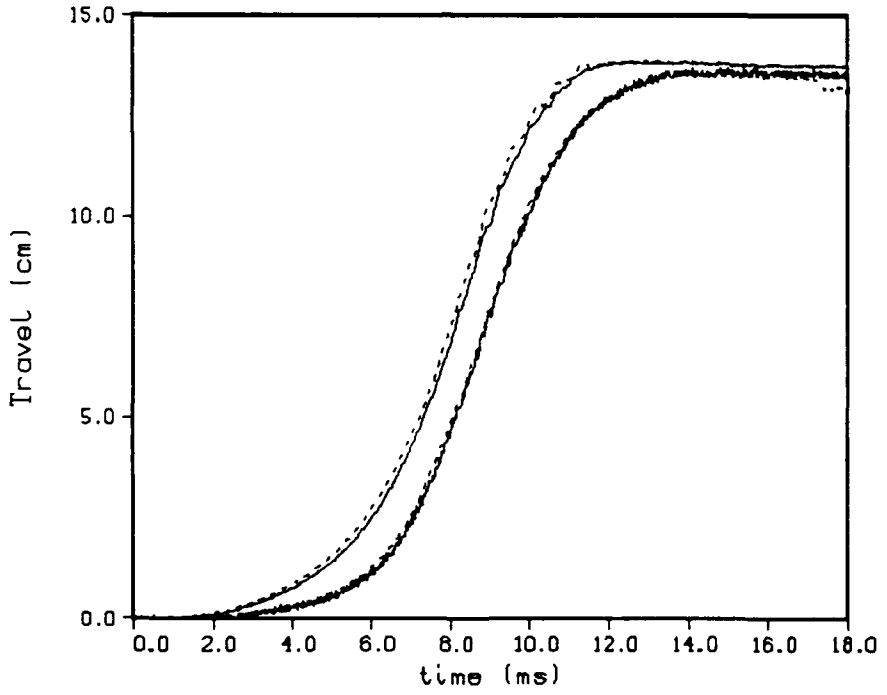

Figure 8. Experimental Piston Travels Minus Recoil. Round 26 (line). Round 18 (dot).

Most of the parameters for the gun code are based on physical measurements of the gun fixture or known propellant or damper fluid properties (see Appendix A). However, some of the parameters cannot be predicted, and the values must be selected based on the experimental data. One parameter that has been studied in the past is the discharge coefficient for the flow out of the propellant reservoir. This can be derived from the experimental chamber and propellant pressures and the experimental piston travels using an inverse code.[7,8] When the vent area changes rapidly, as is the case here, it is clearer to represent the results in terms of effective area (discharge coefficient times vent area).[9] Figure 9 shows the results for shots 26 and 18. In Figure 9, the solid line represents the actual area as derived from the experimental piston travels. The effective area is larger than the actual area from approximately 2 to 10 ms, and it is felt that this result reflects slight discrepancies in the actual piston position. Since both pistons are moving, and the nose of the control piston is slanted, small discrepancies in piston position translate to relatively large changes in the vent area. Also, uncertainties in the pressure data, as seen earlier, induce uncertainty in the derived discharge coefficient for the liquid reservoir. Thus, the results are viewed qualitatively, rather than quantitatively, and simply indicate little flow loss for this fixture from the liquid reservoir to the combustion chamber. Since the effective area is close to the actual area throughout the firing cycle, a value of 0.95 is chosen as the discharge coefficient for flow out of the propellant reservoir. Higher dimensional modeling indicates that this is a good approximation.

A similar analysis can be completed for the damper flow (Figure 10). After some initial noise, the effective area is well below the actual area, indicating flow losses. Near the end of the stroke, the effective area approaches the actual area and becomes larger than the physical area at end of stroke (discharge coefficient larger than one). Near the end of the stroke, the flow pattern becomes more complicated, and a smaller discharge coefficient, to account for greater flow losses, would be expected (see Figure 3). Thus, flow out of the damper appears to be complicated.

GE has constantly modified the damper orifice over the course of the firings to improve the gun performance. The engineering drawings at BRL for the damper profile are out of date, and the profile used here was obtained from GE as a table of vent area vs. distance from end of stroke. The results above indicate there is likely a problem with the vent area table supplied by GE near the end of stroke. Since the vent area is small, a minor measurement error could lead to a fairly large error in the area.

There is another possibility. The transducer block will bend out slightly due to the high damper pressure.[10] Since the vent area is very small, this could create a noticeable effect. Some

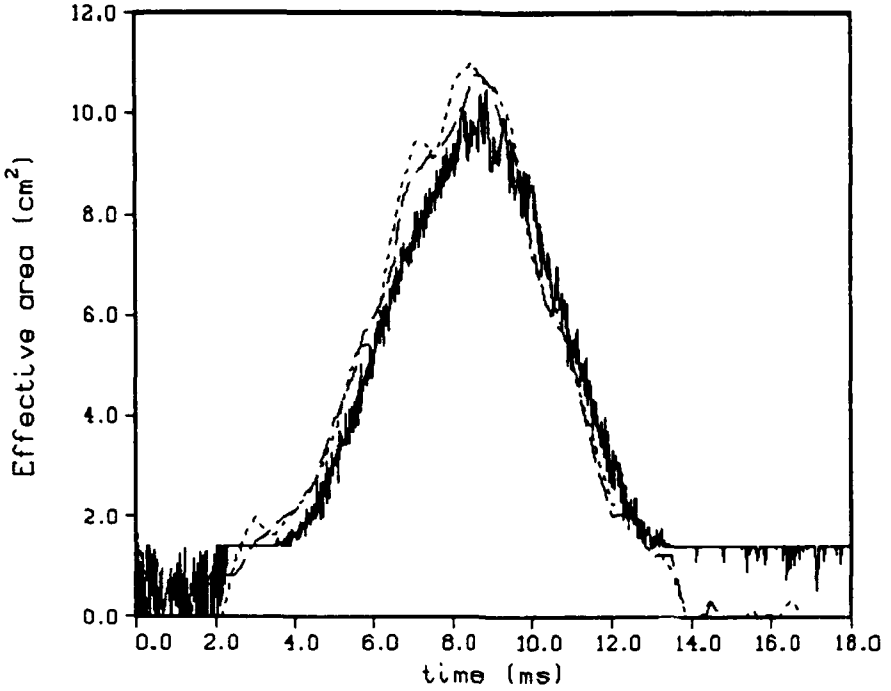

Figure 9. Results From Inverse Code - Reservoir. Injection Area (line). Effective Area - Round 26 (dot) and Round 18 (dash). Based on the Gauges H120 and LP210.

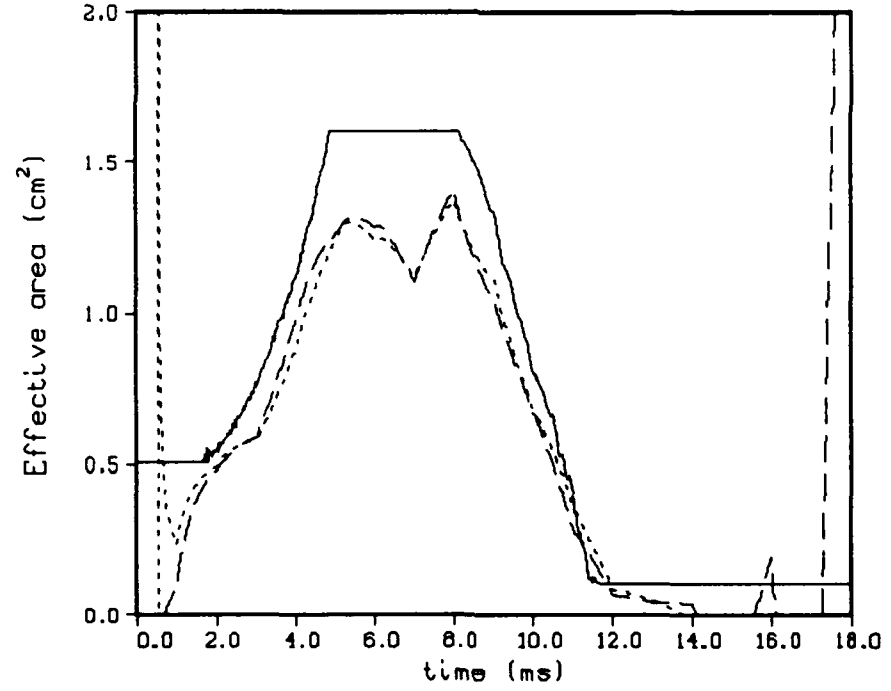

Figure 10. Results From Inverse Code - Damper. Injection Area (line). Effective Area - Round 26 (dot) and Round 18 (dash).

calculations were made using the formula for an infinite thick cylinder. The largest expansion of the vent area was around 5% at the end of stroke. This is substantially smaller than the discharge coefficient overshoot. And the calculation will probably overestimate the displacement of the block since end effects are ignored. So, this effect is considered negligible and ignored in the model.

There is another anomaly in the damper pressure data. The pressure at the end of stroke stays up around 40 MPa, rather than going down to the original damper pressure. Originally, this was also attributed to an error in the vent area. If the vent area actually goes to zero, high pressure liquid will be trapped at the front of the damper, where the pressure gauge is located. The damper pressure will not fall until the chamber pressure becomes low enough to allow the control rod to back up. However, an alternate explanation has been offered.[10] The flow through the narrow orifice will heat the damper fluid. It is known that a small temperature increase will lead to a large pressure increase if the density is kept constant. The amount of heating of the damper fluid is not known and neither is the equation of state, so this cannot presently be quantified. But this is now considered to be the most likely explanation of the pressure behavior. This behavior did not occur for the 30 mm gun fixture because there was a small hole drilled in the front of the damper that allowed the pressure to be relieved.[4]

The damper flow is seen to be more complicated than the propellant injection. Both the transducer block expansion and the temperature related pressure increase will be most important near the end of stroke. However, the exact behavior at the end of stroke will have a minor effect on performance, so the vent area table appears adequate.

The discharge coefficient itself oscillates around 0.8 for a good part of the stroke. It is preferred to use a constant value for the discharge coefficient rather than a profile that changes with time. Therefore, a constant discharge coefficient of 0.8 was initially chosen to represent flow out of the damper based on the experimental pressures and inner piston travel.

A useful option in the gun code is the ability to use the experimental chamber pressure as a boundary condition. This allows a check on the piston motion and injection process without having to consider the combustion process. The code was run using only the experimental chamber pressure H120. The damper pressure and piston travels were predicted by the code. Three different choices for the discharge coefficient out of the damper were made, and the resultant damper pressure and control piston travel with discharge coefficients of 0.75, 0.85, and 0.95 are shown in Figures 11 and 12, respectively. The model damper pressures are uniformly low. The early portion of the model of the damper pressure is almost independent of the choice of discharge

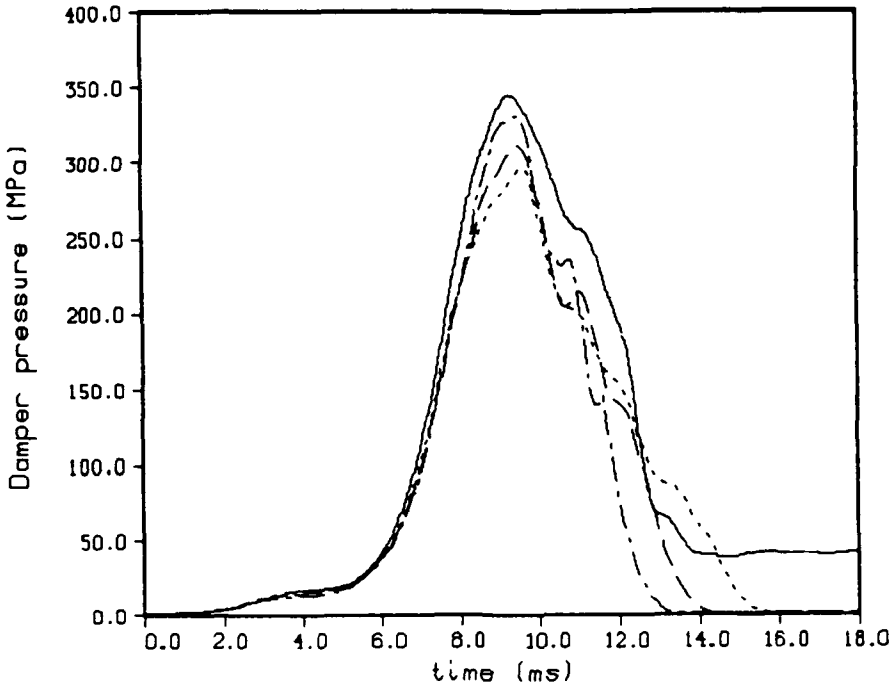

Figure 11. Damper Pressure - Round 26 (line). Model With Chamber Pressure H120. CD_5 = 0.75 (dot). CD_5 = 0.85 (dash). CD_5 = 0.95 (dot-dash).

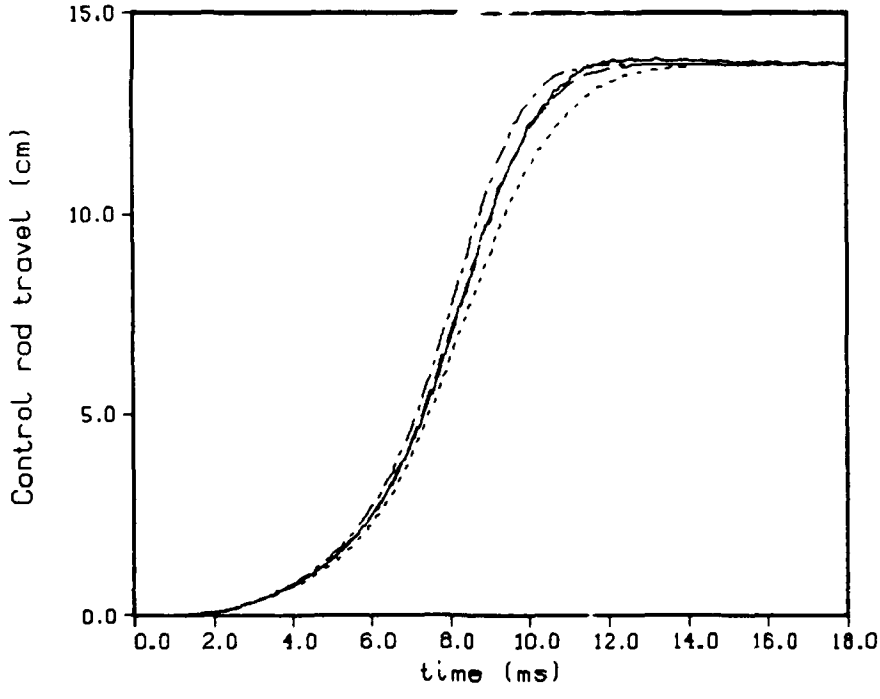

Figure 12. Control Rod Travel - Round 26 (line). Model With Chamber Pressure H120. CD_5 = 0.75 (dot). CD_5 = 0.85 (dash). CD_5 = 0.95 (dot-dash).

coefficient. As the discharge coefficient out of the damper is raised, the control rod moves more rapidly and keeps the damper pressure up. A discharge coefficient of 0.85 gives a control rod (inner piston) travel that matches the experiment almost exactly (see Figure 12). Since the control rod motion controls the vent area, it is considered to be of primary importance in the performance of the gun. Thus, a discharge coefficient out of the damper of 0.85 is chosen to match the control rod travel. This value is a refinement of the 0.8 value for the discharge coefficient discussed above based totally on experimental data. It is noted that, for the 30 mm gun firings, a much smaller discharge coefficient of 0.70 was used. This is reasonable since the vent area of the damper in the 30 mm is much smaller than the 105 mm, and the flow was past a sharper corner.

The shot start pressure is another parameter which is of importance in modeling the 105 mm experiments, and the muzzle velocity is sensitive to changes in shot start pressure. The shot start pressure is derived from the radar for the experiment and is taken to be applied for a distance of 11.5875 cm, the length of the forcing cone obtained from the projectile drawings. Although more complicated resistance profiles are sometimes used, solid propellant modeling suggests that this is a reasonable method of obtaining a resistance profile. A value of 35 MPa for the shot start pressure gives good agreement with the early projectile travel using chamber pressure gauge H120 as a boundary condition. However, the radar is lost after the early travel. Since the gun has a smooth bore, and the resistance pressure after shot start should be small, the resistance pressure after 1.5875 cm of travel is neglected in the modeling which follows.

The gun code, utilizing the chamber pressure gauge H120 as a boundary condition, fails shortly before muzzle exit. The difficulty is that the combustion chamber pressure becomes much lower than the computed gun tube pressure, creating a need for mass flow backwards into the combustion chamber. Since the model allows only mass flow from the combustion chamber into the gun tube, which is the expected physical situation, the solution cannot continue with a reverse flow. The pressure gauges in the combustion chamber and tube have been reported by GE to heat and lose accuracy after peak chamber pressure, resulting in recorded pressures that are too low. It appears likely that gauge drift due to heating occurs in this experiment. The complementary gauge in the combustion chamber, H270, records even lower pressures after maximum chamber pressure, and it is felt to be even less accurate.

To remove the reliance on the experimental pressure, the igniter model is utilized with input values determined by considering experimental shots where water replaces the liquid propellant. The igniter is 168.5 g of IMR4350, although, for simplicity, the model assumes that the igniter is

the same as the liquid propellant. The water shots show a rise time of about 5 ms to a pressure of about 21 MPa, and, thus, the igniter is assumed to be injected at a constant rate to obtain a pressure of 21 MPa at 5 ms. Three-quarters of the igniter energy is assumed to be lost through heat transfer, giving approximately the correct chamber pressure when combustion is shut off in the model. A heat loss of 50% was used in the 30 mm modeling. A more complicated primer model indicates that unburned igniter powder is carried into the chamber.[11] This powder could be cooled by the water and, hence, fail to combust. The igniter then would release more energy in the actual shot than in the water shot, but this is not considered in the model.

To complete the interior ballistic model, the combustion chamber pressure is determined from the mass flux and propellant properties using the derived values for the discharge coefficients and resistance profile discussed above. The simplest approximation is to assume that the liquid combusts instantaneously as it enters the chamber. Results of this model are shown in Figures 13 and 14 with the model curves shifted in time so that the steepest portions of the chamber pressure rise agree. The agreement in the steep pressure rise from 5.0 to 9.0 ms is very good. The early behavior is not reproduced well, indicating that liquid accumulation in the combustion chamber is important in the startup. This inaccuracy is reflected in the lack of agreement in piston travels in Figure 14. The maximum pressure in Figure 13 is, however, quite accurate. After the peak pressure, the model shows much higher pressures than the experiment. The experimental chamber pressures after maximum are probably inaccurate due to gauge drift. This conclusion is substantiated by the predicted muzzle velocity of 658 m/s, which is close to the experimental muzzle velocity of 666 m/s.

To obtain better agreement between the model and experiment, particularly in the piston travels, a droplet model is necessary to account for accumulation of the liquid propellant in the combustion chamber during the startup. In this model, the Sauter mean droplet diameter is input as a function of chamber pressure. The liquid accumulation and the droplet mean diameter can be derived from the inverse code. However, approximations must be made, and the results are even less accurate than the discharge coefficient derivations. Instead, the droplet diameter profile is adjusted by trial and error to match the experimental chamber pressure. The droplet diameter is chosen to be monotonically decreasing, although other possibilities are discussed below. The droplet diameter profile chosen is shown in Table 2. Also, Appendix A shows the input job stream for the droplet model and the summary output page.

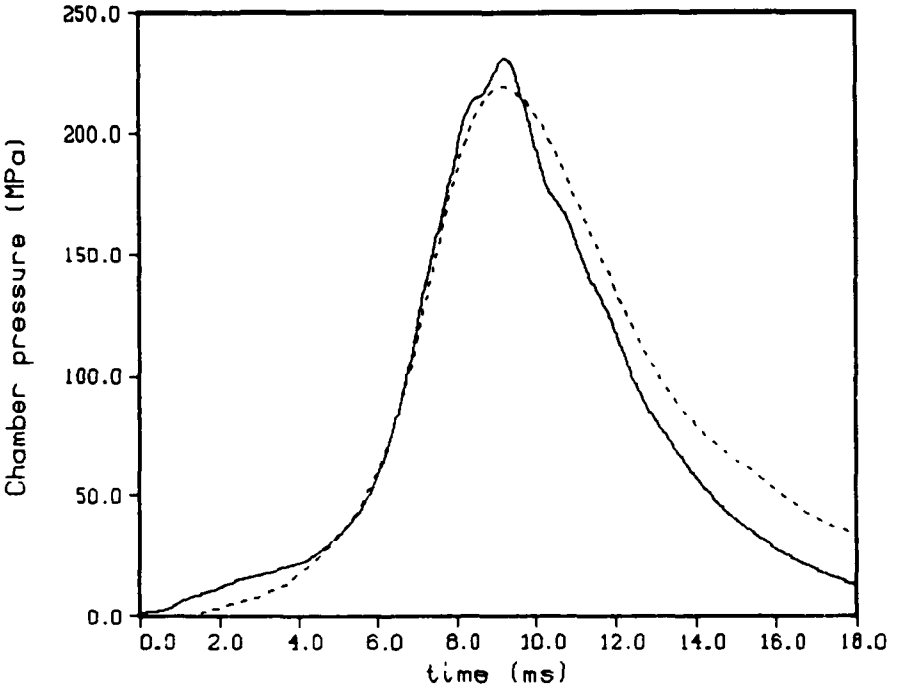

Figure 13. Chamber Pressure - Round 26 - Gauge H120 (line). Model With Instantaneous Burning (dot).

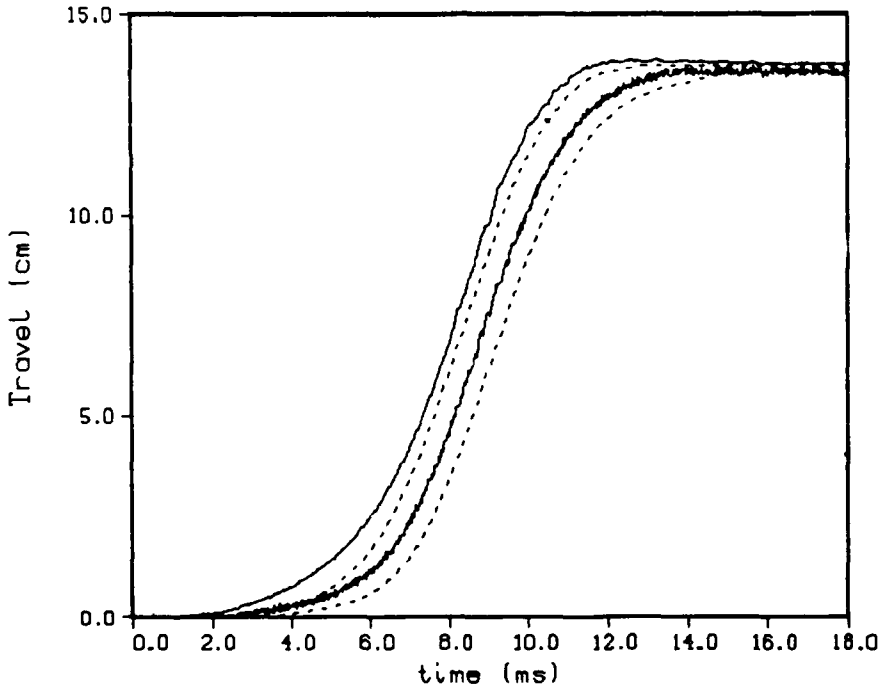

Figure 14. Piston Travels - Round 26 (line). Model With Instantaneous Burning (dot).

TABLE 2. Round 26 Mean Droplet Diameter Profile.

Chamber Pressure, MPa	Droplet Diameter, μm
0.0	250
25.0	250
50.0	100
100.0	75
150.0	50
200.0	25
250.0	10

Figures 15 through 19 compare the model using the input in Appendix A (and droplet model in Table 2) with the experimental pressures and travels. The predicted muzzle velocity is 659 m/s, a -1.1% difference from the experimental value of 666 m/s. It was not possible to match the experimental mean velocity exactly without unreasonable assumptions about heat loss. The chamber pressure must change significantly to affect the muzzle velocity due to the high expansion ratio of 12.3. The expansion ratio is defined as the final free volume (volume in the combustion chamber and tube) divided by the initial free volume (volume in the combustion chamber and liquid reservoir). It is desired to follow the experimental chamber pressure to maximum as closely as possible. Thus, the predicted muzzle velocity is felt to be acceptable since it is within the required 2% window, and the experimental and predicted chamber pressures are in agreement with reasonable physical assumptions. If more of the igniter energy is in fact released later in the firing cycle, this would help match the experimental muzzle velocity.

A closer comparison of the chamber pressure curves shows that the model in Figure 15 follows the higher pressure curve H120 very closely until about 200 MPa. At this point the experimental maximum pressures differ. However, the model maximum pressure must reach the higher of the recorded experimental maximum pressures in order to approach the experimental muzzle velocity. The model liquid pressure in Figure 16 is close to the experimental pressures and agrees well except in the early behavior from 0.0 to 4.0 ms. Although lower than the experiment, the model damper pressure in Figure 17 shows reasonable agreement. The flow out of the damper is likely more complicated than steady state Bernoulli flow with a constant discharge coefficient assumed in the model. However, the piston travels shown in Figure 18 are now very accurate, indicating that the damper model is adequate. The experimental radar trace breaks down at about 9 ms, so the experimental projectile travel is only accurate for early times. The projectile travel agreement shown in Figure 19 is very good for this initial start-up region.

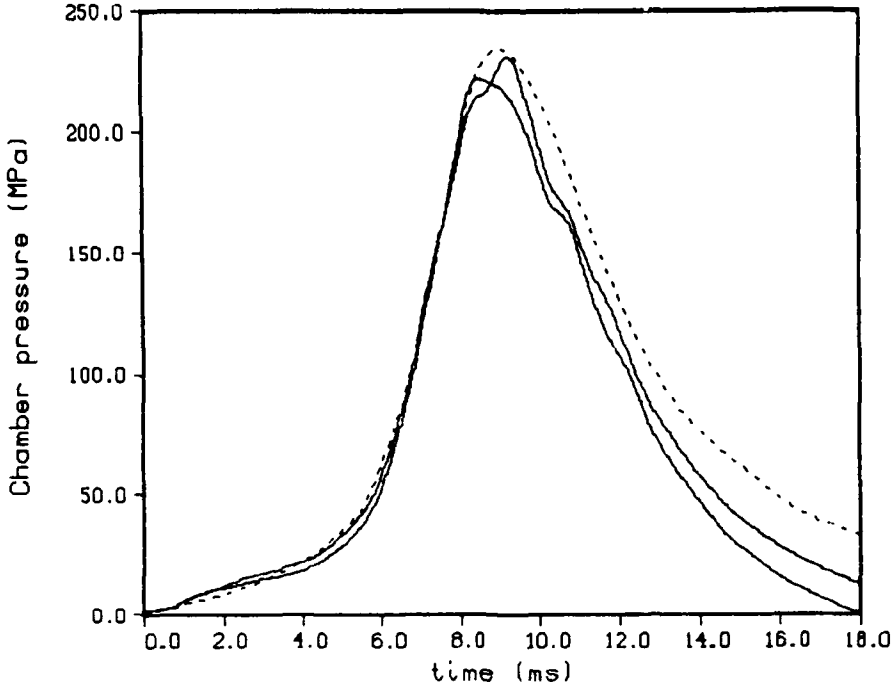

Figure 15. Chamber Pressure - Round 26 (line). Model With Droplet Burning (dot).

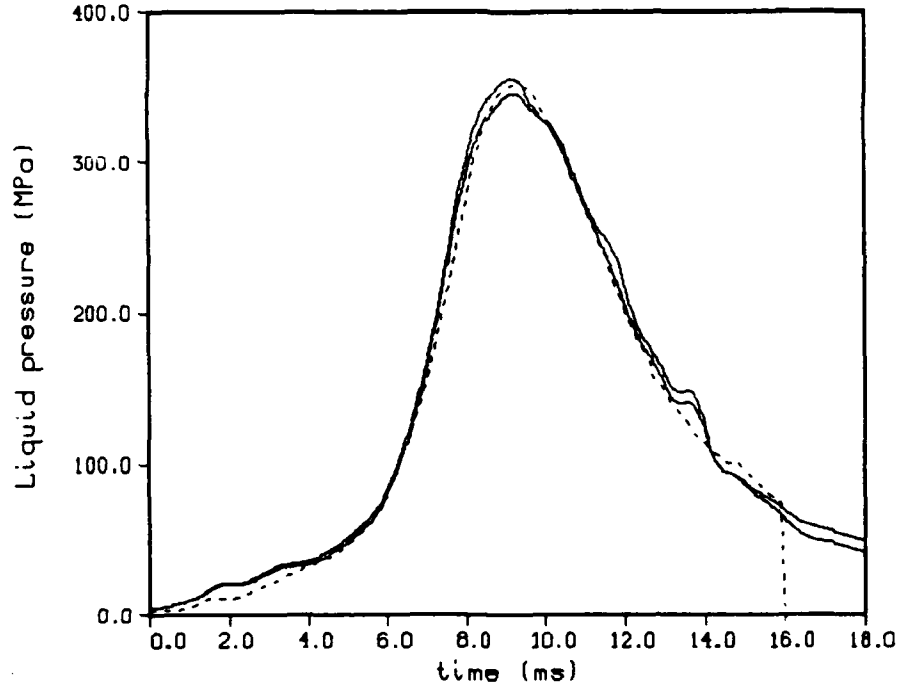

Figure 16. Liquid Pressure - Round 26 (line). Model With Droplet Burning (dot).

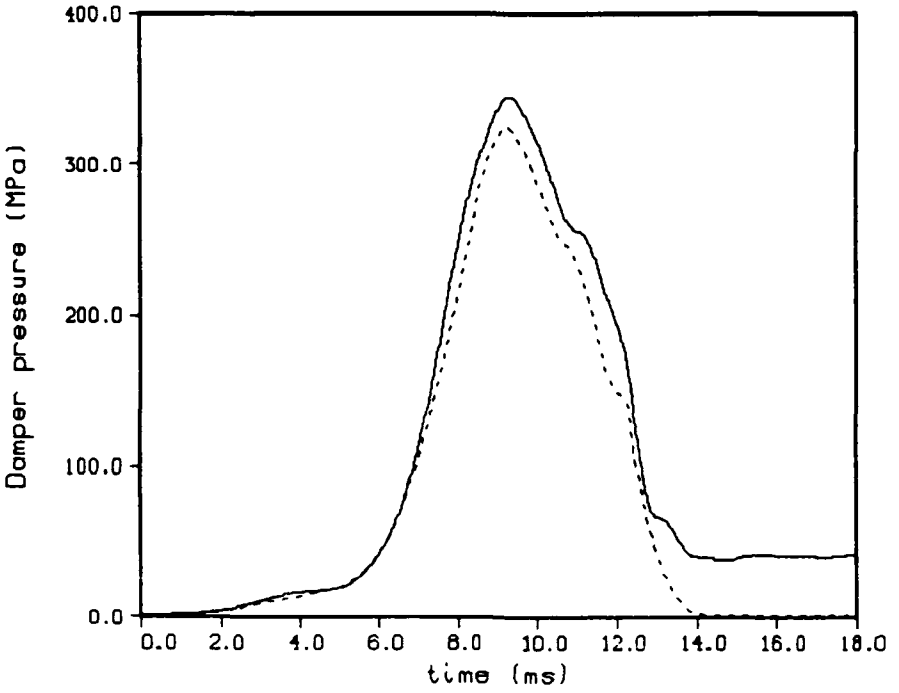

Figure 17. Damper Pressure - Round 26 (line). Model With Droplet Burning (dot).

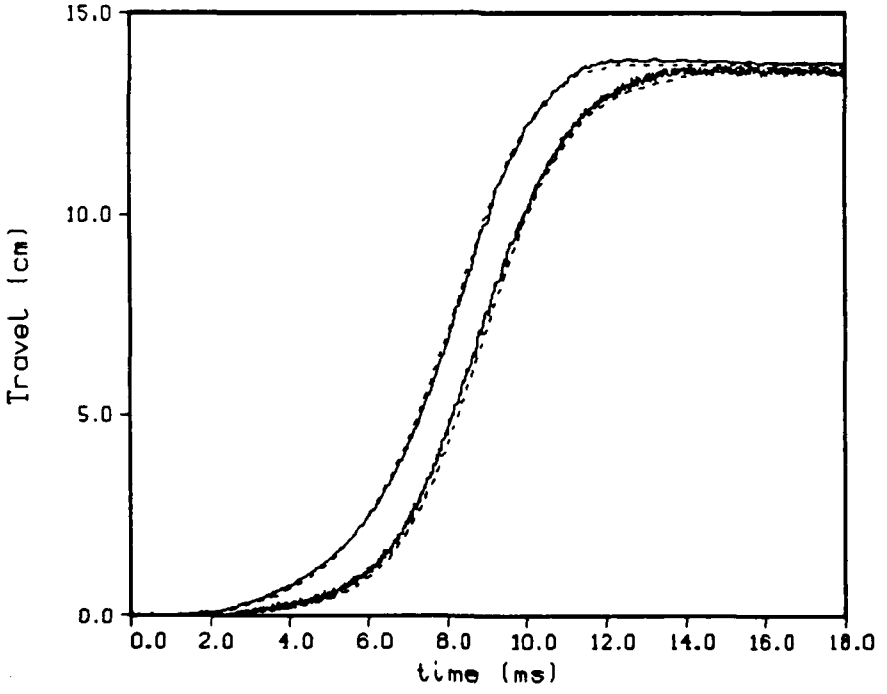

Figure 18. Piston Travels - Round 26 (line). Model With Droplet Burning (dot).

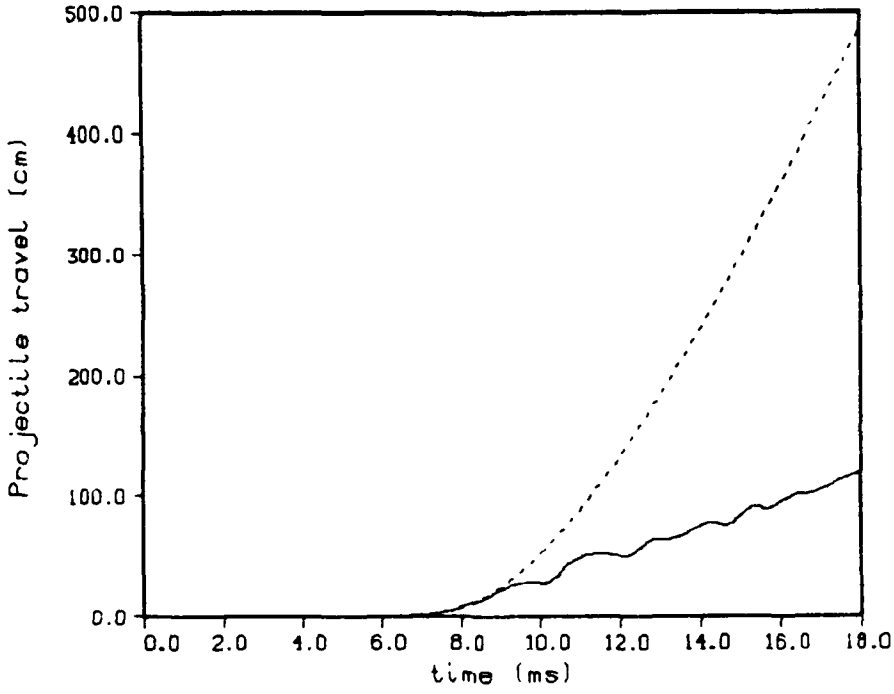

Figure 19. Projectile Travel - Round 26 (line). Model With Droplet Burning (dot).

A review of Figures 15 to 19 shows the largest discrepancy between the model and the experiment is in the chamber pressures after maximum pressure (shown in Figure 15). However, it appears likely that much of the discrepancy is due to gauge drift. After peak pressure, the experimental chamber pressure drops faster than the model allows, even with combustion turned off. While heat loss to the combustion chamber walls (ignored in the model) could cause some pressure drop, this is not expected to be large enough to cause the rapid pressure drop recorded. The model accuracy is partially confirmed by the fact that the liquid pressure curves are matched quite closely in this region. A similar observation was made for the 30 mm data, and it is concluded that gauge drift is a primary suspect for the lack of agreement.

Experimental pressures were also measured at three positions in the gun tube--at 3.06 m and 2.21 m from gun tube muzzle (projectile travel of 487.7 cm) as well as near the end of the tube. The two gauges of interest are shown in Figures 20 and 21. The model and the experiment agree both in magnitude and timing of opening with a faster drop-off in the experiment in Figure 20. The lack of agreement may again be due to gauge drift. This conclusion appears to be substantiated by observing the entire gun tube pressure profile at a late time (Figure 22). Since this is a low performance shot with low muzzle velocity, the model pressure profile is almost flat, as expected. The first experimental value appears to be much too small since the pressure profile is not expected to have as large a slope as indicated by the two data points.

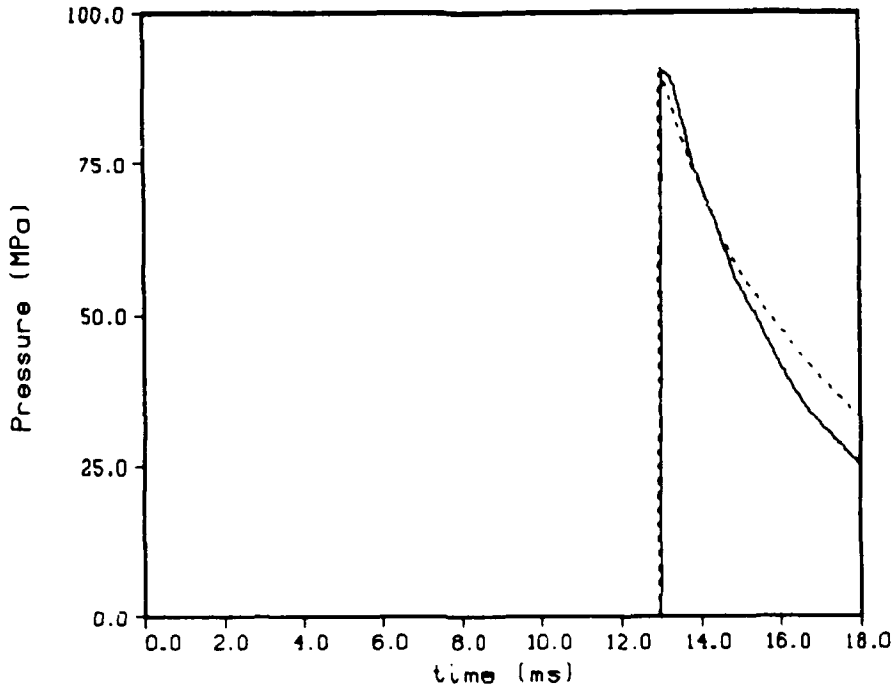

Figure 20. Barrel Pressure 3.06 m From the Gun Tube Muzzle - Round 26 (line). Model With Droplet Burning (dot).

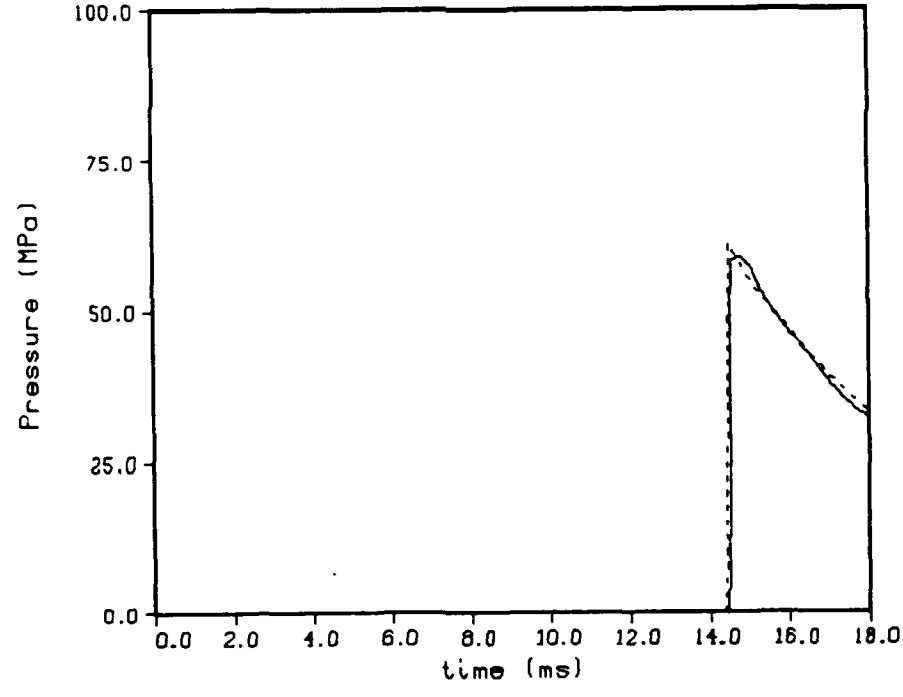

Figure 21. Barrel Pressure 2.21 m From the Gun Tube Muzzle - Round 26 (line). Model With Droplet Burning (dot).

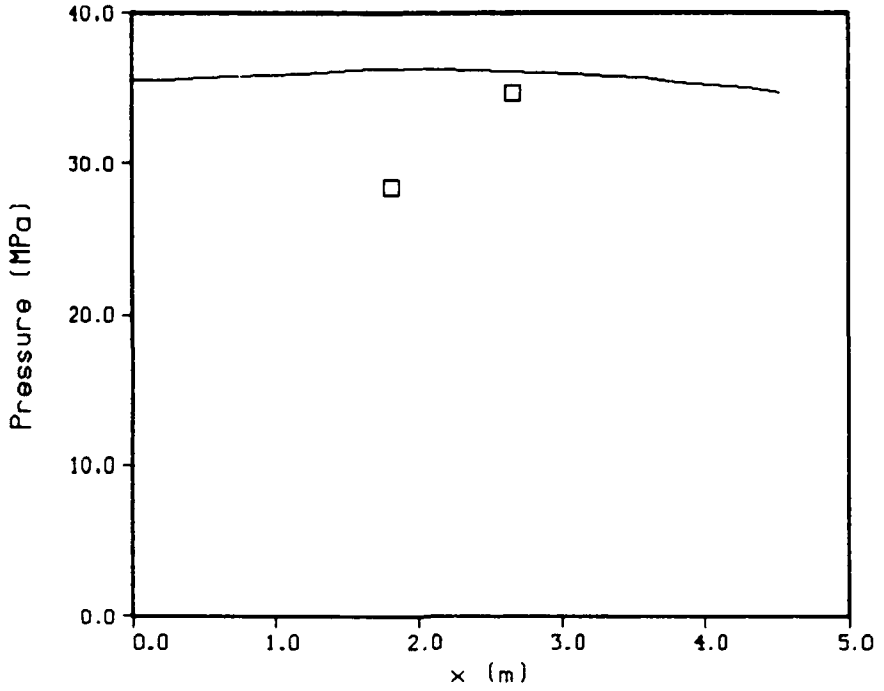

Figure 22. Gun Tube Pressure Profile at 17.5 ms. Round 26 data (squares). Model With Droplet Burning (line).

6. GE 105 MM GUN FIXTURE - OTHER CONFIGURATIONS

Since a match was obtained with experimental data in the repeatability series (long charge), it was of interest to determine if the model could be used in a predictive mode for the two other configurations shown in Table 1. Due to the constant changes in the damper to improve the gun performance, these series were not as repeatable as the long charge series. Instead, individual shots were chosen.

Shot 15 was chosen from the medium charge firings. As indicated in Table 1, compared to the repeatability series, there is less liquid propellant and a larger initial combustion chamber volume. A heavier projectile was used, and the damper was different. After shot 15, the damper was modified to eliminate the sharp corner on the bushing that forms the vent with the damper rod, a change which will modify the discharge coefficient and mass flux. Otherwise, the damper is essentially unchanged. However, because of the shorter stroke in shot 15, only the latter part of the damper profile used for shot 26 is relevant. The experimental muzzle velocity was 539.7 m/s.

Shot 7 was chosen from the short charge firings. There is even less liquid propellant than the medium charge firings and a correspondingly larger initial combustion chamber volume. The damper is different than either the medium or long charges. Instead of the three flats cut into the

damper rod beginning in shot 13 (in which the bushing was also reversed from shots 1-12), two flat regions were cut into the damper rod. Also, the damper rod was not fixed to the control piston (or inner piston) until shot 10. These modifications serve to change the discharge coefficient and mass flux. The experimental muzzle velocity was 391.2 m/s.

The changes in the gun dimensions in terms of liquid reservoir volume, combustion chamber volume, and piston strokes were made in the code. The discharge coefficients and the droplet distribution were left unchanged although the damper orifice had been modified. This allows a comparison of the experiment and the model in a predictive mode. Table 3 shows the resulting muzzle velocities. The agreement between the experiment and the model is better than expected.

TABLE 3. Model With Round 26 Droplet Profile. Muzzle Velocities.

	Experimental, m/s	Model, m/s	% Difference
Round 26	666	659	-1.1
Round 15	540	544	0.7
Round 7	391	395	1.0

Unfortunately, there is not good agreement with the experimental combustion chamber pressure shown in Figures 23 and 24 for shots 15 and 7, respectively. In particular, the model shows much larger peak pressures (of about 15%) than the experiments. The model adequately predicts an integrated quantity like the muzzle velocity but does not reproduce the details of the pressure history. This result is not unexpected due to the expected changes in the discharge coefficient for the damper. A change in the damper discharge coefficient will affect the control piston travel directly, thereby directly altering the delivery of liquid propellant to the combustion chamber. The droplet profile as a function of pressure is expected to change as well since the vent area and chamber conditions now differ.

In fact, it is interesting to run the code assuming that the liquid combusts instantaneously as it enters the chamber. In all three shots (26, 15, and 7), the muzzle velocity is predicted accurately as shown in Table 4. Thus, the droplet profile is only required to match the maximum pressure and the details of the firing cycle for the low performance shots examined in this 105 mm series.

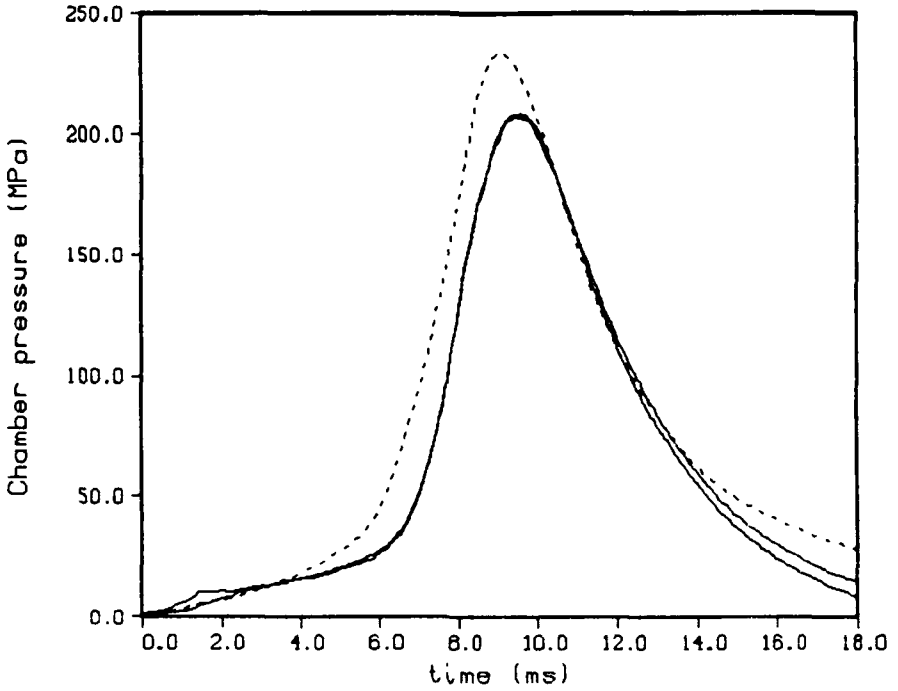

Figure 23. Chamber Pressure - Round 15 (line). Model With Round 26 Droplet Profile (dot).

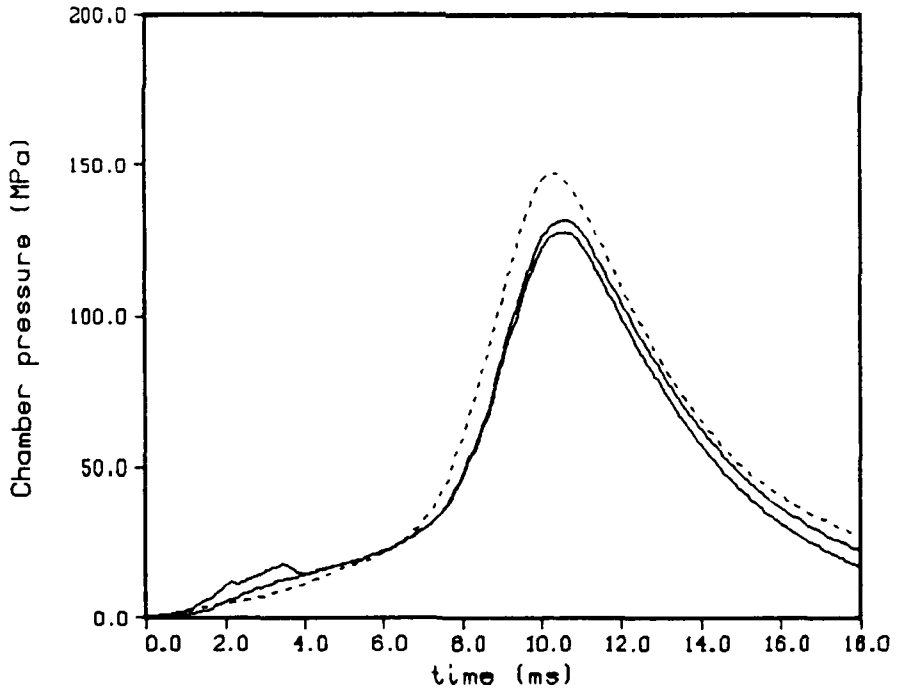

Figure 24. Chamber Pressure - Round 7 (line). Model With Round 26 Droplet Profile (dot).

TABLE 4. Model With Instantaneous Burning. Muzzle Velocities.

	Experimental, m/s	Model, m/s	% Difference
Round 26	666	654	-1.8
Round 15	540	541	0.2
Round 7	391	394	0.8

7. FURTHER MODELING - MEDIUM CHARGE

The parameters derived in the baseline study are adequate for predicting the gross performance of the gun with the medium charge in shot 15. However, it was felt that differences between the values used in the predictive mode and the values required to more accurately represent the experimental data may better illuminate the physics. Thus, new values for the experimental parameters are derived for the medium charge firing.

A review of the experimental data from shot 15 indicates that a value of 0.95 for the discharge coefficient out of the reservoir is reasonable. This is the same value used in the repeatability series modeling, and it was the expected value since the orifice was unchanged. However, examination of the results of a run using the experimental chamber pressure for round 15 indicated that 0.80 is a better value for the discharge coefficient out of the damper than the 0.85 value used in modeling shot 26. This is reasonable since this earlier damper is similar to that in the repeatability series except that it has a sharp corner, which should lead to a smaller discharge coefficient.

A new droplet profile is derived for round 15 (shown in Table 5) with the input parameters detailed in Appendix B. The droplet diameter, in general, must be chosen larger to obtain a longer delay and a smaller peak pressure compared to shot 26. It is possible to match the experimental muzzle velocity exactly and still stay close to the experimental chamber pressure up to the peak as shown in Figure 25. Possible explanations for the lack of agreement in chamber pressures after maximum pressure were discussed previously. The damper pressures shown in Figure 26 agree at the beginning of the firing cycle with some anomaly near peak pressure as well as the usual disagreement near the end of the stroke. In general, the agreement is good.

TABLE 5. Round 15 Mean Droplet Diameter Profile.

Chamber Pressure, MPa	Droplet Diameter, μm
0.0	600
25.0	600
50.0	100
100.0	75
150.0	75
200.0	60

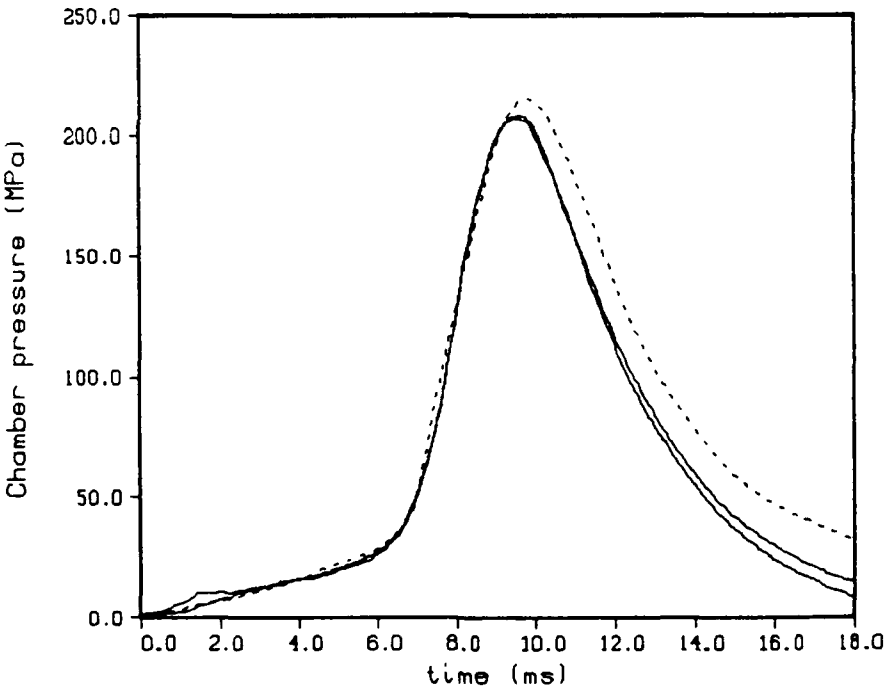

Figure 25. Chamber Pressure - Round 15 (line), Model With New Droplet Profile (dot).

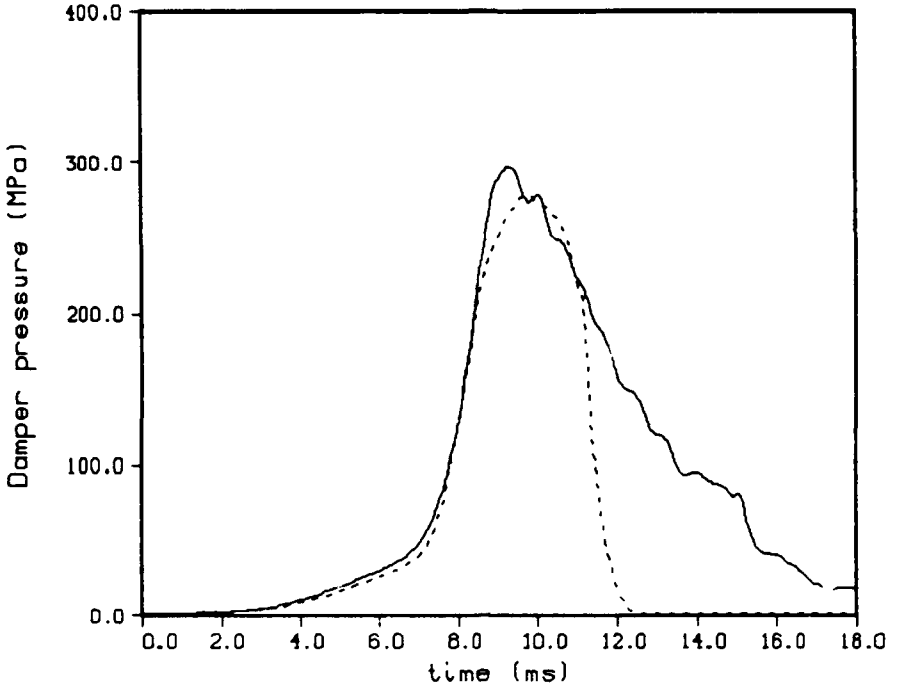

Figure 26. Damper Pressure - Round 15 (line). Model With New Droplet Profile (dot).

The model for shot 7, a short charge, is run with the new droplet profile derived for shot 15, a medium charge. The predicted muzzle velocity is shown in Table 6. The model now predicts a late chamber pressure rise in Figure 27 rather than the early pressure rise using the shot 26 droplet diameter profile in Figure 24. It is not expected that the droplet profile derived from shot 15 would be an improvement in modeling the short charge compared to the shot 26 profile. As indicated previously, the damper is significantly different, and the pressures are lower. Hence, the conditions influencing mass flux and droplet size are significantly different.

8. FURTHER MODELING - SHORT CHARGE

To complete the study of droplet profiles using a constant discharge coefficient of 0.95 for the propellant reservoir (since the injection orifice is unchanged), new values for the discharge coefficient for the damper and a new droplet profile are derived for the short charge. A value of 0.65 agrees with experimental data for the discharge coefficient out of the damper. At this stage in the 105 mm experiments, the damper piston was not fixed to the control rod. Bouncing in the damper pressure trace was observed by GE and given as the reason for fixing the damper rod to the control piston.[5] Vibrations in the damper piston would be expected to disturb the flow, leading to a smaller discharge coefficient than that for shots 15 and 26. In addition, the physical shape of the orifice was different (two flats rather than three as discussed previously), with an unknown effect on the discharge coefficient.

TABLE 6. Comparison of Experimental and Simulated Muzzle Velocities With Droplet Diameter Profile Derived for Shot 15.

	Experimental, m/s	Model, m/s	% Difference
Round 15	540	540	0.0
Round 7	391	396	1.3

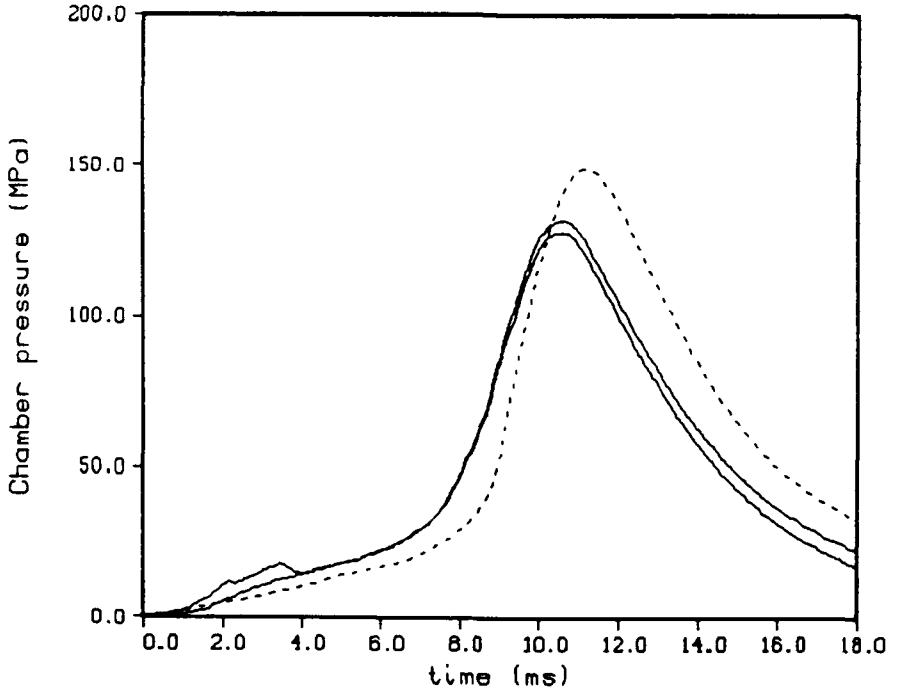

Figure 27. Chamber Pressure - Round 7 (line), Model With Round 15 Droplet Profile (dot).

A new droplet profile was derived for round 7 and is shown in Table 7, with detailed input in Appendix C. The latter droplet diameter must be chosen quite large to prevent the muzzle velocity from becoming too large. It is possible to match the experimental muzzle velocity of 391 m/s exactly and still stay reasonably close to the experimental chamber pressure up to the peak as shown in Figure 28. Again, the drop-off in the experimental chamber pressure compared to the model is evident and is believed to be partly gauge drift. The damper pressures in Figure 29 match fairly well up to peak pressure, with the bouncing noted by GE evident in the pressure trace. In general, the changes in the discharge coefficient for the damper and in the droplet profiles are necessary for a match with model pressures and velocity. However, as noted earlier, the gross behavior of the experiment is predicted by empirical values derived from either shot 26 or 15.

TABLE 7. Round 7 Mean Droplet Diameter Profile.

Chamber Pressure, MPa	Droplet Diameter, μm
0.0	250
25.0	250
50.0	125
100.0	90

9. DISCUSSION: EMPIRICAL PARAMETERS

Although the model presented above demonstrates excellent agreement with the experimental data, values of the empirical parameters of discharge coefficients for the propellant reservoir, the damper, and the mean droplet diameter distribution are derived from the experimental data. A long term goal of liquid propellant interior ballistic modeling is the prediction of performance for a gun design. Thus, it is desirable to obtain values of these parameters which are independent of a particular fixture.

A combination of the values of the discharge coefficients (for the reservoir and the damper) and the droplet profile determines both the mass flux of the liquid propellant into the combustion chamber and the surface area available for combustion. Since the model utilizes a pressure-dependent burn rate law based on strand burner experiments for LGP1845, the droplet profile

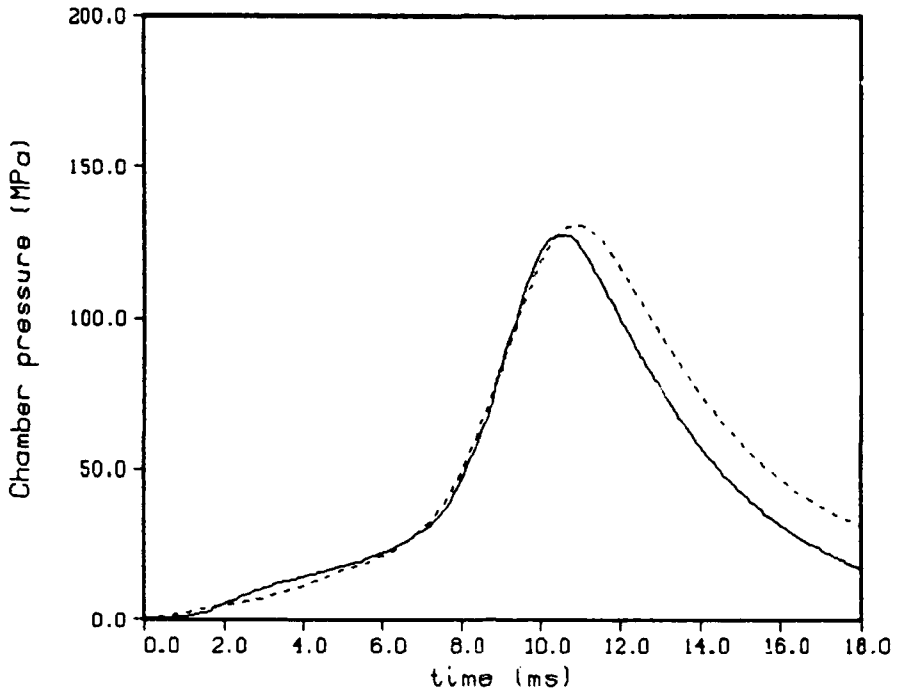

Figure 28. Chamber Pressure - Round 7 (line). Model With New Droplet Profile (dot).

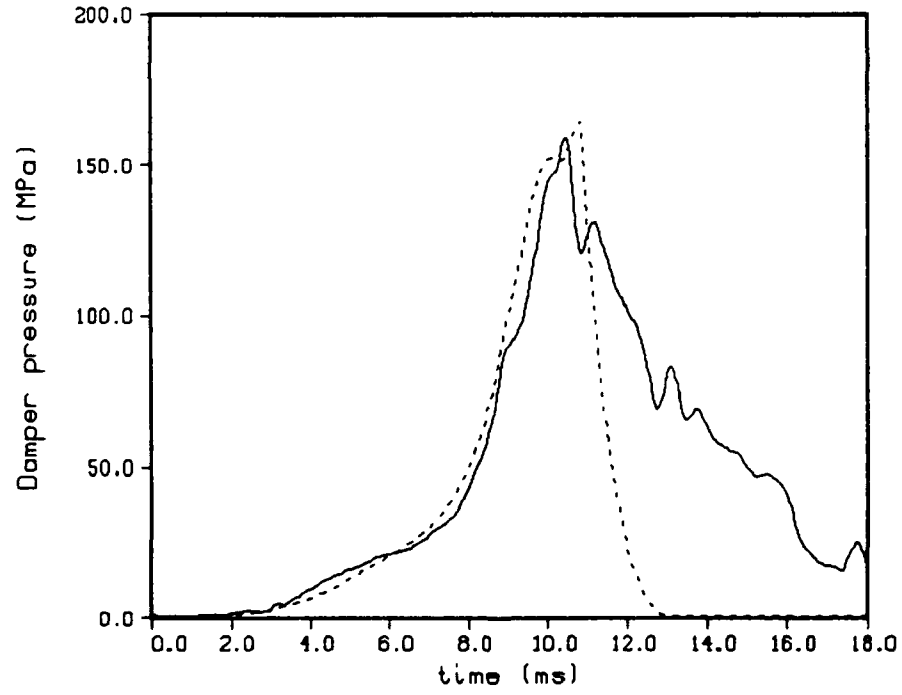

Figure 29. Damper Pressure - Round 7 (line). Model With New Droplet Profile (dot).

determines the mass generation rate. Although the discharge coefficients are taken to be constant, it is noted that the vent area changes constantly, particularly during the initial startup. Thus, one would expect that during the opening of the vent from the closed position to fully open, the discharge coefficient would change as well due to the inertia of the liquid. Also, one would expect the geometry of the orifice to influence the discharge coefficient, and, in the case of the damper, the orifice geometry has varied substantially. The droplet diameter profile is dependent upon the amount of mass introduced into the combustion chamber (that is, the surface area necessary to match a given chamber pressure is dependent upon the amount of mass in the chamber). Thus, it is indirectly dependent upon the discharge coefficients. The simple assumptions utilized to match the experimental data are known to be an approximation. Therefore, in an effort to obtain an indication of the interdependence of these parameters and relax the assumption of constant discharge coefficients, they were varied as detailed below.

The inverse code was utilized as detailed below with the higher of the chamber and liquid pressures for shot 26. The recorded piston travels provide a measure of the increase in volume in the combustion chamber. Projectile travel and the resulting increase in volume for gas expansion is obtained from the radar for 0.0 to 9.0 ms, after which the radar signal is lost.

First, the inverse code is utilized to suggest a droplet profile from the experiment. The mean droplet diameter is derived from the liquid accumulation (defined as the total mass of liquid in the combustion chamber and tube which has been injected but has not released energy). The liquid accumulation is based on the conservation equations for mass and energy. The predicted mean droplet diameter was obtained from both chamber pressure gauges presented earlier and found to be consistent.

The initial liquid accumulation from the inverse code in Figure 30 is negative from 0.0 to 4.0 ms. The negative accumulation may be the result of lack of detail in the igniter model. If the igniter injects more gas earlier in the experiment than the model predicts, less liquid is required to augment the pressure, and, hence, less accumulation is observed. Another possibility is inaccuracy in the pressure gauge. If the gauge registers an experimental pressure which is too high, more gas is needed than is available to produce the pressure. Thus, the model would create gas by generating negative accumulation. In any case, the data in Figure 30 for the first four milliseconds are not physically meaningful.

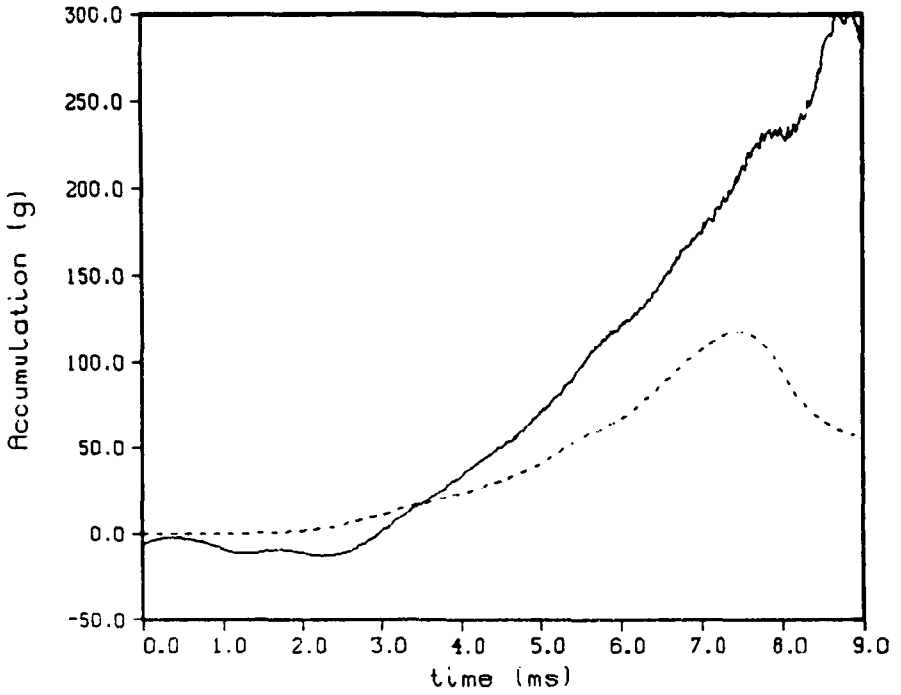

Figure 30. Liquid Accumulation. From Experiment (line). From Droplet Burning Model (dot).

By four milliseconds, the pistons have moved noticeably (see Figure 18), and the igniter is contributing an increasingly smaller percentage of the pressure. Thus, the liquid accumulation in Figure 30 and the corresponding Sauter mean diameter in Figure 31 are more meaningful. The solid line in the figures represents the values derived from the experimental measurements by the inverse code while the dotted line represents the profile used to match the experimental data as shown in Figures 15-22 (in which the initial droplet size is arbitrarily chosen). The experimental accumulation (initial propellant mass of 2815.67 g) and the corresponding mean droplet diameter are substantially larger than that used previously. The differences are due to small changes in the piston travel. For this fixture, 1.0 mm of piston travel corresponds to about 20 g of liquid propellant injected. Slight changes in the piston travel can be caused by small changes in the damper model.

The final jump in accumulation from 7.0 to 9.0 ms in the inverse code is due to the leveling off of the experimental pressure just after 7.0 ms for one of the pressure gauges (as seen in Figure 15). This leveling of the pressure is unexpected and, in fact, is not recorded by the other chamber pressure gauge in Figure 15. Thus, the recorded pressure for this gauge and the resulting rise in accumulation from 7.0 to 9.0 ms is questionable. From 6.0 to 9.0 ms in Figure 31, the experimental mean droplet diameter drops as the accumulation burns off.

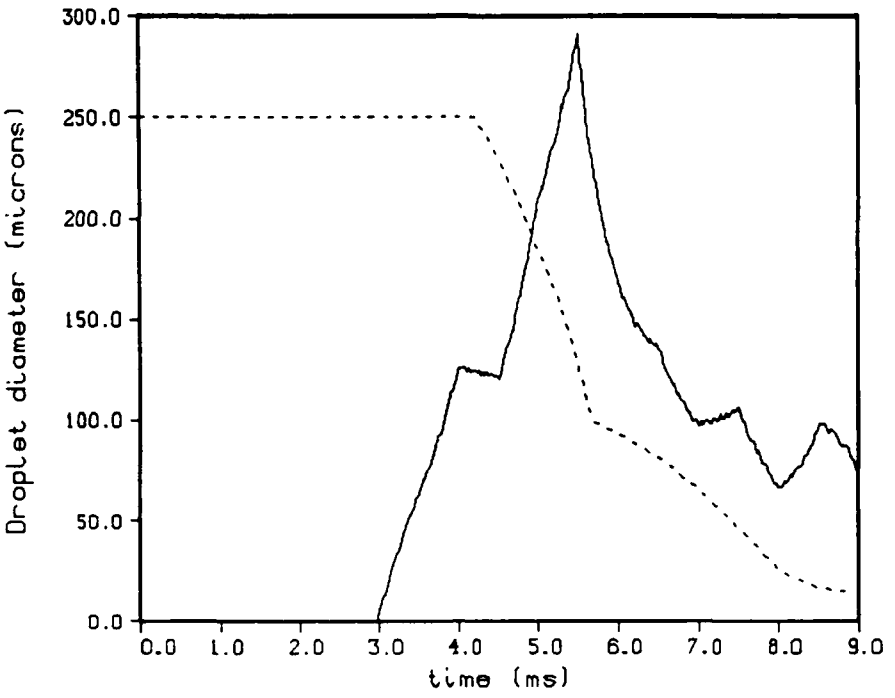

Figure 31. Droplet Diameter. From Experiment (line). From Droplet Burning Model (dot).

A comparison of the experimental values and the values chosen previously suggests that the scenarios of liquid breakup are different. The dotted curves in Figures 30 and 31 suggest initial large droplets, somewhat arbitrarily chosen for the small amount of liquid in the chamber, which decrease in size to a small droplet diameter at maximum chamber pressure near 9.0 ms. The experimental values suggest an initial fine spray with small droplets which increase in size as the vent opens fully near 6.0 ms, after which breakup is more efficient as the chamber pressure rises. The droplet diameter drops during the steep pressure rise from 6.0 to 9.0 ms. However, the droplets remain relatively large, and accumulation continues to increase. Qualitatively, the droplet sizes in Figure 31 agree over the steep portion of the pressure rise from 6.0 to 9.0 ms.

Although the previously chosen values for the droplet profile are adequate to describe the data using the constant values of the discharge coefficients for the propellant reservoir and damper, it is instructive to utilize the droplet profile predicted above by the inverse code to examine jet breakup. As a first step, the constant values of the discharge coefficients of 0.95 for the propellant reservoir and 0.85 for the damper are used. The resulting chamber pressure is shown in Figure 32, where an initial droplet diameter of 10 μm was used in place of the negative values. The comparison with the experimental chamber pressure shows that the small droplets from 4.0 to 6.0 ms cause the pressure to be too large, while the large droplets from 6.0 to 9.0 ms cause the pressure to be too low.

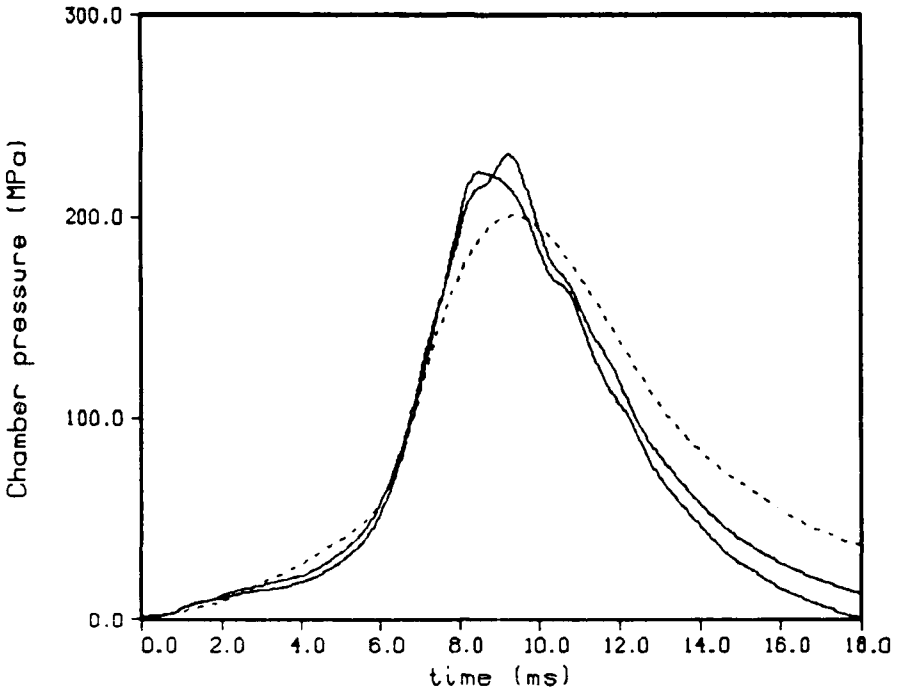

Figure 32. Chamber Pressure. Round 26 (line). Model - Inverse Code Droplet Profile (dot).

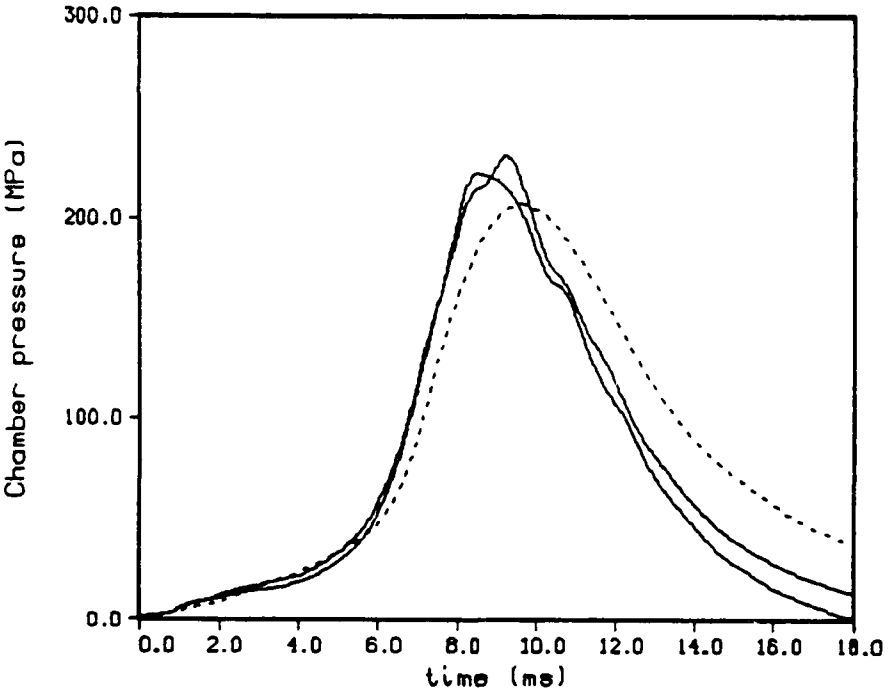

Figure 33. Chamber Pressure. Round 26 (line). Model - Inverse Code Droplet Profile - Smaller Reservoir Discharge Coefficient (dot).

Since a constant value of the discharge coefficient for the reservoir is known to be an approximation, and smaller values are suggested by the experimental data during the initial startup, the discharge coefficient is taken to be 0.5 for the first 1.5 mm of piston travel (after which it is returned to the 0.95 value). The result is shown in Figure 33 for the chamber pressure. The early comparison from 0.0 to 6.0 ms is now improved; however, the later behavior in the model pressure from 6.0 to 9.0 ms is now further from the experiment.

Therefore, to match the later behavior of the pressure curves using the inverse droplet diameter profile, it appears necessary to inject more liquid. The discharge coefficient for the reservoir is already large at 0.95, and increasing it further has only a minor effect. Another way to inject more liquid is to increase the discharge coefficient for the damper since the control piston will move faster in response. The result of changing the discharge coefficient for the damper from 0.85 to 0.95 and maintaining the constant discharge coefficient of 0.95 for the propellant reservoir is shown in Figures 34 and 35. Although the chamber pressures in Figure 34 are now in much better agreement, the comparison with piston travels in Figure 35 shows that the control piston (or inner piston) moves too quickly.

Thus, the experimental chamber pressure data are not well modeled using the inverse droplet diameter profile and manipulating the discharge coefficients, a result contrary to a similar application for the 30 mm data. However, slight errors in the piston travels or experimental pressures will alter the derived droplet diameter profile. Also, approximations in the igniter model and damper model affect the predicted chamber pressure.

It is also of interest to compare the derived droplet diameter profiles from the three 105 mm cases discussed in this report (shots 7, 15, and 26). The comparison is shown in Figures 36 and 37 as mean droplet diameter vs. time and chamber pressure, respectively. As discussed previously, negative values of the mean droplet diameter are physically meaningless and indicate error in either the pressure measurement or the primer model. In any case, the amount of liquid injected, as derived from the piston travel measurements, is about 0.06% and 0.35%, respectively, of the total for the first 3 ms for shots 26 and 15, and about 1.99% of the total for the first 4 ms in shot 7. The differences in time (shown in Figure 36) are not unexpected since the pressure-time histories of the three shots are quite different in the initial startup regimes. The pressurization rates in Figures 15, 25, and 28 reflect the changes in initial combustion chamber volume shown in Table 1, the larger initial volume associated with the short charge (shot 7) taking longer to pressurize.

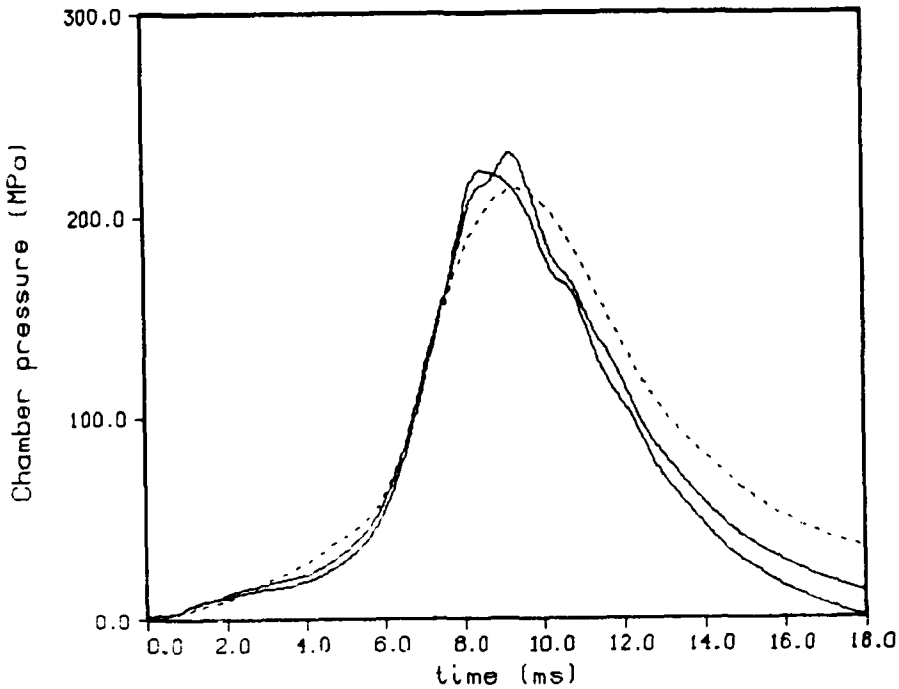

Figure 34. Chamber Pressure. Round 26 (line). Model - Inverse Code Droplet Profile - Larger Damper Discharge Coefficient (dot).

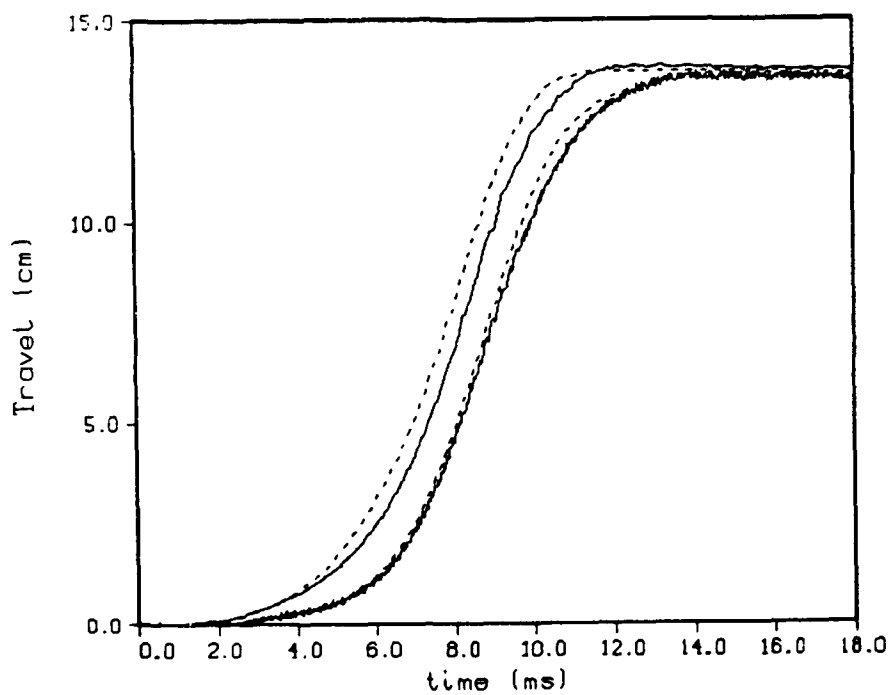

Figure 35. Piston Travels. Round 26 (line). Model - Inverse Code Droplet Profile - Larger Damper Discharge Coefficient (dot).

The comparison of mean droplet diameter derived from the inverse code with pressure is shown in Figure 37. Unfortunately, the droplet diameters are not reconciled. Although the general shape of the curves is similar (initial small droplets followed by an increase in droplet size as the vent opens with a decrease as combustion becomes vigorous), the predicted sizes are relatively quite different. The differences may be due to changes in the amount of propellant injected, small errors in experimental measurement, or a fundamentally different jet breakup in the three cases. In fact, at 50 MPa, 6.9% of the liquid propellant has been injected in shot 26, 15.3% in shot 15, and 25.5% in shot 7. Thus, it is not surprising that the droplet diameters are not reconciled with pressure. However, it is possible that the total surface area available for combustion is roughly the same, even with the differences in droplet diameter.

As a final comparison, the mean droplet diameters used with the constant discharge coefficients in Figures 15, 25, and 28 with time and pressure are shown in Figures 38 and 39. Although there is weak similarity between the graphs (which has been somewhat artificially imposed), the mean droplet diameters utilized are different.

Thus, it will be necessary to consider parameters other than mean droplet diameter to reconcile the data from the three 105 mm firings discussed in this report with a single combustion model. Some possibilities include a consideration of other chamber and entrance conditions such as vent area. Also, it may be necessary to breakdown the mean droplet diameter into the component parts of mean diameter of incoming liquid and mean diameter of previously injected liquid.

10. DISCUSSION: SENSITIVITY ANALYSIS

To obtain an estimate of the sensitivity of the mean droplet diameter profile to changes in several initial conditions, the following cases were considered. The analysis is performed for the baseline shot 26 parameters with the constant discharge coefficients. The five cases are:

A. The baseline round 26 droplet model.

B. The reservoir discharge coefficient was changed from 0.95 to 0.90.

C. The damper discharge coefficient was changed from 0.85 to 0.90.

D. The shot start pressure was changed from 35 MPa to 40 MPa.

E. The primer injection time was changed from 5.0 to 6.0 ms.

A new droplet profile was derived for the four new cases (Table 8). The sensitivity is similar to the 30 mm case.

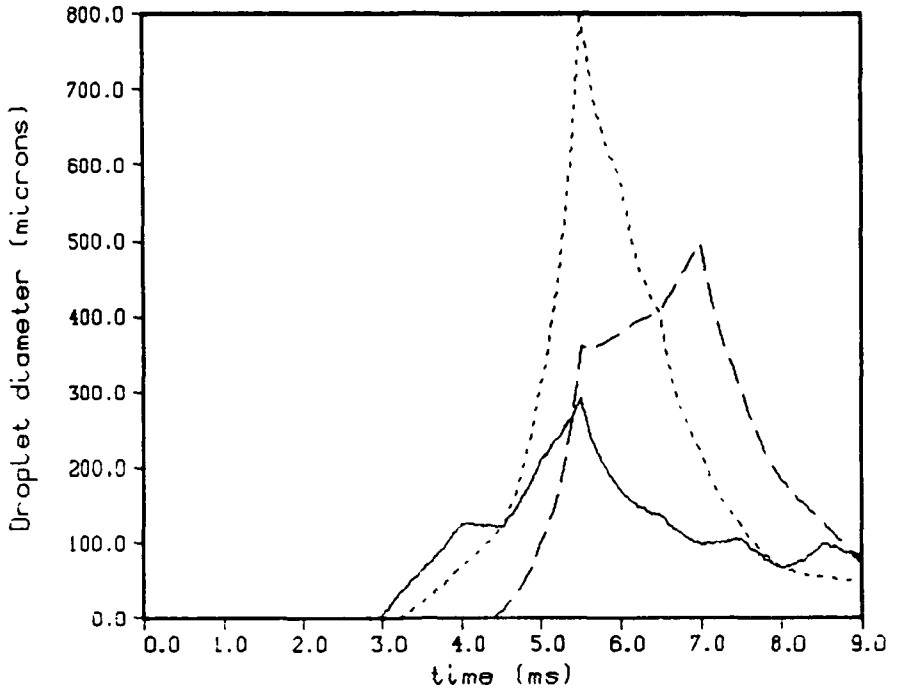

Figure 36. Droplet Diameter From Inverse Code vs. Time. Round 26 (line). Round 15 (dot). Round 7 (dash).

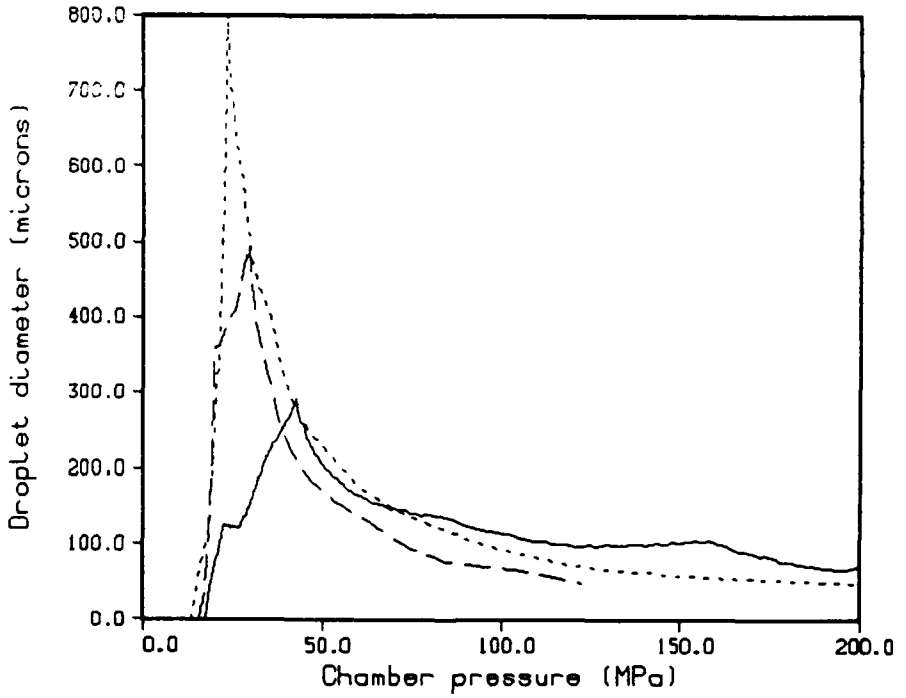

Figure 37. Droplet Diameter From Inverse Code vs. Pressure. Round 26 (line). Round 15 (dot). Round 7 (dash).

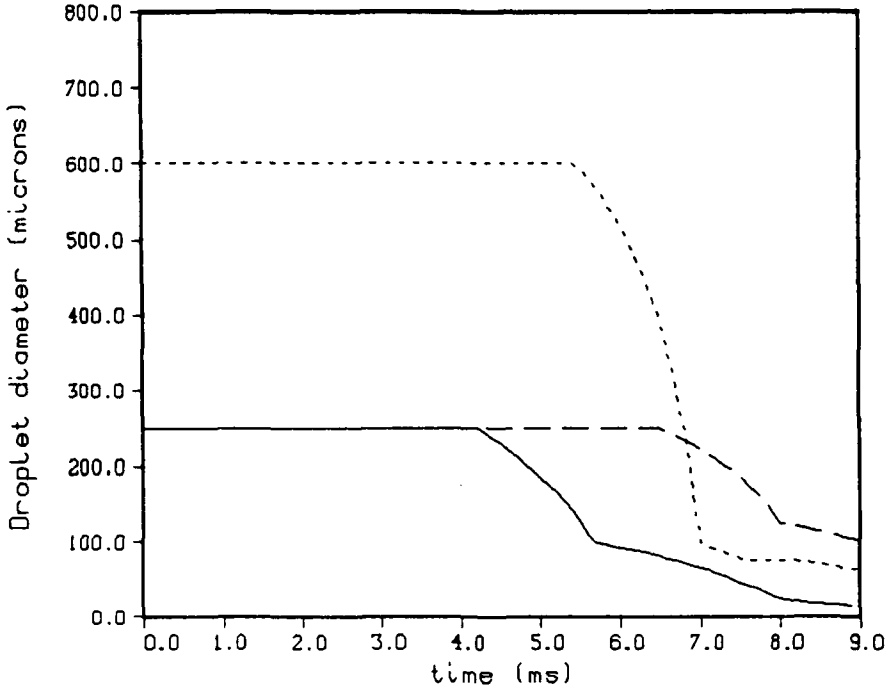

Figure 38. Droplet Diameter From Model Runs vs. Time. Round 26 (line). Round 15 (dot). Round 7 (dash).

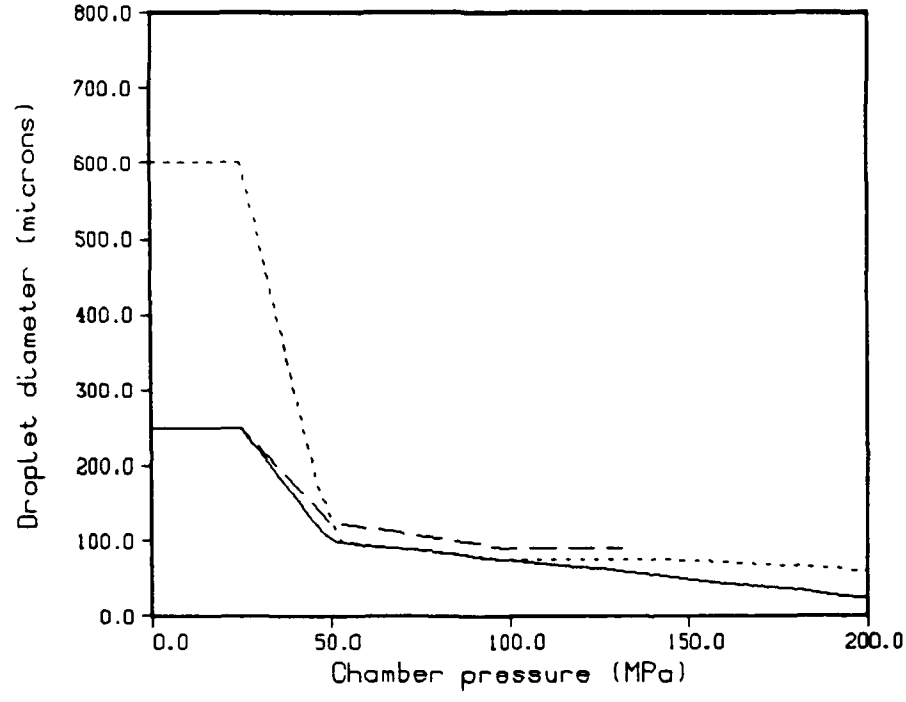

Figure 39. Droplet Diameter From Model Runs vs. Pressure. Round 26 (line). Round 15 (dot). Round 7 (dash).

Table 8. Sensitivity Analysis - Mean Droplet Diameter Profiles (microns).

Pressure, MPa	A	B	C	D	E
0	250	250	250	250	150
25	250	250	250	250	150
50	100	100	125	125	75
100	75	75	85	85	40
150	50	40	60	60	25
200	25	20	30	30	5
250	10	10	25	30	5
v_m	659	658	663	660	659

Unlike the 30 mm case discussed in a previous report,[4] it was possible to reproduce the chamber pressure for each of the above cases. As before, the mean droplet diameter is most sensitive to changes in the primer model. Unfortunately, the droplet diameter profile is not unique.

11. CONCLUSIONS

A model has been developed for the Concept VIC regenerative liquid propellant gun which incorporates the major features of the gun in a lumped parameter form. Most of the needed parameters are physical dimensions of the gun and properties of the propellant which can be chosen without reference to experimental firing data. However, parameters which must be benchmarked from a study of the data are the discharge coefficient out of the propellant reservoir, the discharge coefficient out of the damper, and the droplet diameter profile.

A constant discharge coefficient of 0.95 for the propellant reservoir appears reasonable for all the VIC firings studied so far (30 mm and 105 mm). The damper has a smaller vent and a more complicated flow pattern than the propellant reservoir. Since the geometry of the damper is varied, the discharge coefficient out of the damper varies from case to case and is in the 0.7 to 0.85 range for the cases considered. However, it has been possible to assume a constant discharge coefficient for the dampers studied. The mean droplet diameter also varies. There are no obvious correlations for droplet diameter, but it undoubtedly depends on the damper as well as the piston assembly. It would be more informative to make a series of shots with different charge lengths but

using the same damper. Since the damper assembly has been constantly changed, this type of information is not yet available.

The model is able to match experimental data from the 105 mm Concept VIC RLPG using reasonable values for the parameters which must be empirically determined. Using the model in a predictive mode with parameters determined from the benchmark case, configurations in which the charge size and initial combustion chamber volume have been substantially changed are modeled within the 1% range in velocity and 10% range in pressure-time history. In fact, assuming instantaneous combustion results in predicted muzzle velocities within 2% of the experimental muzzle velocities, in part due to the low performance regime and the high expansion ratio.

A closer prediction of the maximum pressures and the shape of the pressure curves requires a droplet model. The appropriate droplet model varies from case to case depending on the initial assumptions. A consideration of the mean droplet diameter with either time or pressure is not sufficient to reconcile the 105 mm data with a single combustion model. Thus, it appears necessary to consider parameters other than simply mean droplet diameter for accurate prediction.

INTENTIONALLY LEFT BLANK.

12. REFERENCES

1. "Regenerative Liquid Propellant Gun Technology Transition Criteria," Meeting of LP management detailing transition criteria from BRL to ARDEC. Picatinny Arsenal, NJ, November 1988.

2. Coffee, T.P. "A Lumped Parameter Code for Regenerative Liquid Propellant Guns." BRL-TR-2703, U.S. Army Ballistic Research Laboratory, Aberdeen Proving Ground, MD, December 1985.

3. Coffee, T.P. "An Updated Lumped Parameter Code for Regenerative Liquid Propellant In-Line Guns." BRL-TR-2974, U.S. Army Ballistic Research Laboratory, Aberdeen Proving Ground, MD, December 1988.

4. Coffee, T.P., G.P. Wren, and W.F. Morrison. "A Comparison Between Experiment and Simulation for Concept VIC Regenerative Liquid Propellant Guns, I. 30 mm." U.S. Army Ballistic Research Laboratory report, to be published.

5. Magoon, I., A. Maynard, and L. Walter. "Preliminary Report on Test Firings of a 105 mm Regenerative Gun." Paper presented at the 25th JANNAF Combustion Meeting, NASA Marshall Space Flight Center, Huntsville, AL, October 1988.

6. Magoon, I., A. Maynard, and L. Walter. "Test Report on 105 mm Concept VIC," General Electric Company, Draft Report, May 1988.

7. Coffee, T.P. "The Analysis of Experimental Measurements on Liquid Regenerative Guns." BRL-TR-2731, U.S. Army Ballistic Research Laboratory, Aberdeen Proving Ground, MD, May 1986.

8. Coffee, T.P. "Injection Processes in Liquid Regenerative Propellant Guns." BRL-TR-2846, U.S. Army Ballistic Research Laboratory, Aberdeen Proving Ground, MD, August 1987.

9. Bulman, M. "Regenerative Liquid Propellant Tank Guns." Preliminary Status Report, General Electric, Pittsfield, MA, August 1987.

10. Magoon, I., General Electric Company, private communication, August 1989.

11. Luu, M., General Electric Company, private communication, August 1989.

INTENTIONALLY LEFT BLANK.

APPENDIX A:
INPUT AND OUTPUT FILES - ROUND 26

INTENTIONALLY LEFT BLANK.

Below is a listing of the job stream for the baseline model (round 26 - droplet burning). The numbers and labels at the left are read in by the code. The comments at the right are for identification by the user and do not effect the actual code. Following is the summary sheet from the output file. A description of the input and a brief description of the source for the input variables are given first.

The first line is merely a label. It lists the file name of the input job stream and a brief description of the problem.

The initial offset of the projectile and the total distance traveled by the projectile before muzzle exit are given. The diameter of the gun tube is given. The projectile and piston weights (measured by GE) are entered.

The initial volume of the liquid reservoir is given. GE reports a volume of 1974 cc and a piston stroke of 5.38 in (13.665 cm). With the above liquid volume, the gun code generates a piston stroke of 13.687 cm. The initial gas volume is as reported by GE. The initial areas of the reservoir (including control piston) and chamber are derived from the engineering drawings.

The VENT4 option is chosen (VIC gun). The control rod radius vs. relative piston motion is gotten from the drawings. The zero point is where the outer piston and control piston first fit together. The positive direction is to the left (direction of the piston stroke). In this case, only the parts of the control piston to the right (negative direction) are relevant since the outer piston cannot move to the left with respect to the control rod. The area of the hole in the outer piston is computed from the engineering drawings. There is a small grease dyke on this piston.

The piston resistance is set to zero since this is not usually large enough to be important. The discharge coefficient into the chamber is set at a constant 0.95 (see discussion in report). The discharge coefficient into the gun tube is set equal to one (no losses).

The flow into the chamber is modeled as steady state Bernoulli flow (FLUX1). There is only one vent hole. The piston thickness is irrelevant for this option. The flow into the gun tube is steady state isentropic flow (FLUX2).

The shot start pressure is applied over a distance equal to the length of the forcing cone. The value of 35 MPa gives very good agreement with the early projectile travel, using the chamber

pressure H120 as a boundary condition. After shot start, the resistance pressure is set equal to zero. Since this is a smooth bore gun, the resistance pressure should be small.

Next, the physical properties of the propellant HAN1846 are given.

The liquid is pre-pressurized to 3.445 MPa. The initial chamber pressure is 1 atm.

The droplet diameter is read in as a function of chamber pressure (DROP4). The burning rate is read as a two-part function. There is some evidence that there is a break in the slope of the burning rate just under 100 MPa. However, since the rate at higher than 100 MPa is not known, the rate that was measured for lower pressures is used. The code does allow a two-part burning rate to be entered. The droplet diameter table has been chosen to match the chamber pressure.

The igniter is injected in the form of hot gas (PRIM3). The actual igniter mass is 168.5 g. From the water shots, the primer pressurizes the chamber in about 5.0 ms. A heat loss factor of 0.26 is used. That is, only 26% of the energy of the primer actually pressurizes the combustion chamber. This gives about the right chamber pressure if the gun code is run without combustion.

The default models for the heat loss to the gun tube and the air shock are used. Heat loss to the combustion chamber walls is ignored.

The most complicated Lagrange model (TUBE4) is chosen. The model will take into account the rarefaction wave after burnout of the propellant.

The damper or buffer model is chosen (BUFF2). The areas of the damper side of the control rod and the hole in the block are from the engineering drawings. The discharge coefficient is set equal to 0.85 (see discussion in report). The initial volume is estimated from the drawings. The damper is originally pressurized to 1.7225 MPa to reduce ullage. The damper fluid is Brayco 783, which has a density of 0.8885 g/cc. Unfortunately, the bulk modulus for the damper fluid has not been measured. The bulk modulus for a similar fluid, Brayco 750, has been measured up to 21 MPa. This is fit by a linear function to obtain the derivative of the bulk modulus with respect to pressure. This means that the bulk modulus of the damper fluid is uncertain, especially at high pressures.

The vent area is given as a function of control piston travel. The bolt on the back of the control rod has been cut to make this vent. Three flat surfaces are cut on the bolt. The engineering drawings are not up to date, so a table of vent area vs. distance from the end of stroke (supplied by GE) is used.

The code will print out results every 0.1 ms (TINC). Because the code must often change the time step, it is more efficient to restrict the maximum time step (HTOP). The error controls EPS and SREC are given typical values.

The integration method flag MF is set to 22 (backwards differentiation formulas with an internally computed Jacobian). KWRITE is set to zero to eliminate diagnostic messages. A time limit of TMAX is set. If the code takes longer than TMAX seconds to execute, the code will stop gracefully and write the usual summary pages.

The code is only to be integrated once (REP1), and the chamber pressure will be computed normally (CHAM1).

```
dt26 - VIC - Full Charge - Drop - CD=0.95 - CD5=0.85
   0.0        487.7          offset   proj travel
  10.5                       gun tube diameter
 17500.                      proj weight
 22910.                      piston weight
 1974.       1901.          vl   v3
  182.54      248.00        al   a3
vent4                       moving central bolt
   18                          bolt radius versus piston travel
     -4.4450      3.0480
     -0.6274      3.7922
     -0.3734      3.8151
     -0.1194      3.8151
      0.0000      3.8735
      0.8433      4.2850
      1.2700      4.2850
      1.3005      4.0665
      1.3640      3.9116
      1.4275      3.8100
      1.4910      3.7363
      1.5545      3.6779
      1.6180      3.6297
      1.6815      3.5890
      1.8085      3.5331
      1.9355      3.5027
      2.0625      3.4925
     13.6652      3.4925
 47.1365       1.132         ahole    agres
   12300                     rodwt
pis1                        piston resistance
   2
    0.0      0.0
    1.0      0.0
dis1                        dis. coeff. versus piston travel
   2
    0.0     .95
    1.0     .95
dis1                        dis. coeff. vs. proj travel - tube
   2
    0.0    1.0
  487.7    1.0
flux1                       steady state mass flux formulation
   1           1.0            nvo   pth
flux2                       isentropic flow into tube
proj1                       proj resistance
   4
     0.0        35.0
     1.5875     35.0
     1.6         0.0
   487.7         0.0
  1.43   5350.0   9.11     rh0   k1   k2
  4035.5      1.2226       energy    gamma
    66.9      .04988       surface tension   kinematic viscosity
```

```
  22.848       .677          mol wt gas     covolume
   3.445        0.1          p1   p3
drop4                        droplets
  0.01      95.2590          ddr     pbr
  1.64        .103           adrl    bdrl
  1.64        .103           adrl    bdrl
    8
   0.0         .0250
  25.0         .0250
  50.0         .0100
 100.0         .0075
 150.0         .0050
 200.0         .0025
 250.0         .0010
1000.0         .0010
prim3                        inject hot gas
 168.5  0.005   0.26         primer mass  inject time  heat loss
heat1                        no heat loss to chamber walls
heat2                        heat loss to gun tube walls
   300.0    1.0               tube temp   fudge factor
shock2                       air shock
    0.1    300.                airp   airt
    1.4     28.84              airgam airmw
tube4                        unsteady lagrange distribution
burn
buff2                        buffer - brayco 783
  38.320   6.493    0.0      apis   ahole   acir
    .85                      cd5
  524.                       v5
   1.7225   1.7225           p5    pout5
   0.8885  1600.  11.3       rh0   k1   k2
   0.0  1.4   0.727  0.0     eps5  gam5  cv5  b5
   13                        nrat
    0.0000    0.5103
    0.0508    0.5103
    1.3208    1.6075
    7.3048    1.6075
    9.3368    1.4193
   10.9878    1.1036
   12.1308    0.8261
   12.7658    0.6570
   13.1468    0.4912
   13.3259    0.3859
   13.4770    0.2647
   13.6548    0.1212
   13.6870    0.1061

  1.00e-04    1.00e-05      tinc  htop
  1.00e-05    1.00e-08      eps   srec
  22   0                    mf     kwrite
    120.0                   tmax
repl                         integrate once
cham1                        compute p3
```

muzzle vel (m/sec)	659.4
max v pis (m/sec)	30.2
max p1 (mpa)	351.6
max p3 (mpa)	234.3
max p5 (mpa)	324.6
max p1 (mpa)	228.9
max pr (mpa)	226.3
max acc (k-g)	11.3
max mass error	0.01 %
max energy error	0.13 %
ballistic efficiency =	33.37 %
expansion ratio =	12.26
loss to tube walls =	6.22 %

run time = 26.0 nstep = 5261

APPENDIX B:

INPUT AND OUTPUT FILES - ROUND 15

INTENTIONALLY LEFT BLANK.

Below is a listing of the job stream for round 15 with droplet burning. Only the parameters that have been changed from the baseline case are described.

A heavier projectile is used. The initial liquid propellant volume is smaller, and the initial chamber volume is larger.

A new droplet profile has been derived. The discharge coefficient out of the damper has been reduced to 0.80. The initial volume of the damper is reduced. The damper profile is different, primarily because of the different starting position.

```
du15 - VIC - Med - Drop - CD=0.95 - CD5=0.80
   0.0        487.7          offset   proj travel
  10.5                       gun tube diameter
 19600.                      proj weight
 22910.                      piston weight
 1312.       2278.          vl   v3
  182.54      248.00        al   a3
vent4                        moving central bolt
   18                           bolt radius versus piston travel
     -4.4450      3.0480
     -0.6274      3.7922
     -0.3734      3.8151
     -0.1194      3.8151
      0.0000      3.8735
      0.8433      4.2850
      1.2700      4.2850
      1.3005      4.0665
      1.3640      3.9116
      1.4275      3.8100
      1.4910      3.7363
      1.5545      3.6779
      1.6180      3.6297
      1.6815      3.5890
      1.8085      3.5331
      1.9355      3.5027
      2.0625      3.4925
     13.6652      3.4925
 47.1365       1.132         ahole    agres
    12300                    rodwt
pis1                         piston resistance
   2
    0.0      0.0
    1.0      0.0
dis1                         dis. coeff. versus piston travel
   2
    0.0     .95
    1.0     .95
dis1                         dis. coeff. vs. proj travel - tube
   2
    0.0    1.0
  487.7    1.0
flux1                        steady state mass flux formulation
   1           1.0             nvo   pth
flux2                        isentropic flow into tube
proj1                        proj resistance
   4
     0.0        35.0
     1.5875     35.0
     1.6         0.0
   487.7         0.0
  1.43   5350.0   9.11      rh0   k1   k2
  4035.5      1.2226        energy   gamma
    66.9      .04988        surface tension   kinematic viscosity
```

```
  22.848       .677          mol wt gas     covolume
   3.445        0.1          p1   p3
drop4                        droplets
  0.01      95.2590          ddr     pbr
  1.64        .103           adrl    bdrl
  1.64        .103           adrl    bdrl
    7
    0.0         .0600
   25.0         .0600
   50.0         .0100
  100.0         .0075
  150.0         .0075
  200.0         .0060
 1000.0         .0060
prim3                        inject hot gas
 168.5  0.005   0.26         primer mass   inject time   heat loss
heat1                        no heat loss to chamber walls
heat2                        heat loss to gun tube walls
   300.0    1.0               tube temp   fudge factor
shock2                       air shock
    0.1    300.                airp   airt
    1.4     28.84              airgam airmw
tube4                        unsteady lagrange distribution
burn
buff2                        buffer - brayco 783
  38.320   6.493    0.0      apis   ahole   acir
    .80                      cd5
  371.                       v5
   1.7225   1.7225           p5    pout5
   0.8885  1600.  11.3       rh0   k1   k2
   0.0  1.4   0.727  0.0     eps5  gam5  cv5  b5
    9                        nrat
    0.0000    1.5948
    2.8308    1.5948
    4.8628    1.4034
    6.5138    1.0844
    7.6568    0.8133
    8.2918    0.6379
    8.6728    0.4784
    9.0030    0.2711
    9.0972    0.1816
  1.00e-04    1.00e-05       tinc  htop
  1.00e-05    1.00e-08       eps   srec
  22   0                     mf     kwrite
    120.0                    tmax
repl                         integrate once
cham1                        compute p3
```

muzzle vel (m/sec)	540.0
max v pis (m/sec)	22.0
max p1 (mpa)	328.7
max p3 (mpa)	215.3
max p5 (mpa)	281.1
max p1 (mpa)	212.4
max pr (mpa)	210.9
max acc (k-g)	9.4
max mass error	0.01 %
max energy error	0.09 %
ballistic efficiency =	37.72 %
expansion ratio =	13.03
loss to tube walls =	6.49 %

run time = 24.5 nstep = 5334

APPENDIX C:
INPUT AND *OUTPUT FILES* - ROUND 7

INTENTIONALLY LEFT BLANK.

Below is a listing of the job stream for round 7 with droplet burning. Only the parameters that have been changed from the round 15 model above are described.

The initial liquid propellant volume is even smaller, and the initial chamber volume is correspondingly larger.

A new droplet profile has been derived. The discharge coefficient out of the damper has been reduced to 0.65. The initial volume of the damper is reduced. The damper profile is completely different. The damper is pre-pressurized to a slightly lower pressure.

```
dv07 - VIC - Short - Drop - CD=0.95 - CD5=0.65
   0.0        487.7          offset   proj travel
  10.5                       gun tube diameter
 19600.                      proj weight
 22910.                      piston weight
  656.       3409.           vl   v3
  182.54      248.00         al   a3
vent4                        moving central bolt
   18                           bolt radius versus piston travel
     -4.4450      3.0480
     -0.6274      3.7922
     -0.3734      3.8151
     -0.1194      3.8151
      0.0000      3.8735
      0.8433      4.2850
      1.2700      4.2850
      1.3005      4.0665
      1.3640      3.9116
      1.4275      3.8100
      1.4910      3.7363
      1.5545      3.6779
      1.6180      3.6297
      1.6815      3.5890
      1.8085      3.5331
      1.9355      3.5027
      2.0625      3.4925
     13.6652      3.4925
 47.1365       1.132         ahole    agres
   12300                     rodwt
pis1                         piston resistance
   2
    0.0      0.0
    1.0      0.0
dis1                         dis. coeff. versus piston travel
   2
    0.0     .95
    1.0     .95
dis1                         dis. coeff. vs. proj travel - tube
   2
    0.0    1.0
  487.7    1.0
flux1                        steady state mass flux formulation
   1           1.0             nvo   pth
flux2                        isentropic flow into tube
proj1                        proj resistance
   4
     0.0        35.0
     1.5875     35.0
     1.6         0.0
   487.7         0.0
  1.43   5350.0   9.11      rh0   k1   k2
  4035.5      1.2226        energy   gamma
    66.9     .04988          surface tension   kinematic viscosity
```

```
  22.848       .677          mol wt gas     covolume
   3.445        0.1          p1   p3
drop4                        droplets
  0.01      95.2590          ddr     pbr
  1.64         .103          adrl    bdrl
  1.64         .103          adrl    bdrl
     5
    0.0         .0250
   25.0         .0250
   50.0         .0125
  100.0         .0090
 1000.0         .0090
prim3                        inject hot gas
 168.5  0.005   0.26          primer mass   inject time   heat loss
heat1                        no heat loss to chamber walls
heat2                        heat loss to gun tube walls
   300.0    1.0                tube temp   fudge factor
shock2                       air shock
    0.1    300.                 airp   airt
    1.4     28.84               airgam airmw
tube4                        unsteady lagrange distribution
burn
buff2                        buffer - brayco 783
  38.320   6.493    0.0      apis   ahole   acir
    .65                      cd5
  226.                       v5
   0.896    0.896           p5    pout5
   0.8885  1600.  11.3       rh0   k1   k2
   0.0  1.4   0.727  0.0     eps5  gam5  cv5  b5
   8                         nrat
    0.0000    1.5425
    0.2629    1.5150
    1.9139    1.2758
    3.0569    1.0366
    3.6919    0.7974
    4.0729    0.5582
    4.4031    0.3190
    4.5490    0.1410
  1.00e-04    1.00e-05       tinc  htop
  1.00e-05    1.00e-08       eps   srec
  22   0                     mf     kwrite
    120.0                    tmax
repl                         integrate once
cham1                        compute p3
```

muzzle vel (m/sec)	391.5
max v pis (m/sec)	9.7
max p1 (mpa)	202.3
max p3 (mpa)	131.2
max p5 (mpa)	163.1
max p1 (mpa)	130.4
max pr (mpa)	129.9
max acc (k-g)	5.8
max mass error	0.03 %
max energy error	0.03 %
ballistic efficiency =	39.66 %
expansion ratio =	11.50
loss to tube walls =	7.39 %

run time = 20.0 nstep = 5434

No of Copies	Organization
1	Office of the Secretary of Defense OUSD(A) Director, Live Fire Testing ATTN: James F. O'Bryon Washington, DC 20301-3110
2	Administrator Defense Technical Info Center ATTN: DTIC-DDA Cameron Station Alexandria, VA 22304-6145
1	HQDA (SARD-TR) WASH DC 20310-0001
1	Commander US Army Materiel Command ATTN: AMCDRA-ST 5001 Eisenhower Avenue Alexandria, VA 22333-0001
1	Commander US Army Laboratory Command ATTN: AMSLC-DL Adelphi, MD 20783-1145
2	Commander US Army, ARDEC ATTN: SMCAR-IMI-I Picatinny Arsenal, NJ 07806-5000
2	Commander US Army, ARDEC ATTN: SMCAR-TDC Picatinny Arsenal, NJ 07806-5000
1	Director Benet Weapons Laboratory US Army, ARDEC ATTN: SMCAR-CCB-TL Watervliet, NY 12189-4050
1	Commander US Army Armament, Munitions and Chemical Command ATTN: SMCAR-ESP-L Rock Island, IL 61299-5000
1	Commander US Army Aviation Systems Command ATTN: AMSAV-DACL 4300 Goodfellow Blvd. St. Louis, MO 63120-1798

No of Copies	Organization
1	Director US Army Aviation Research and Technology Activity Ames Research Center Moffett Field, CA 94035-1099
1	Commander US Army Missile Command ATTN: AMSMI-RD-CS-R (DOC) Redstone Arsenal, AL 35898-5010
1	Commander US Army Tank-Automotive Command ATTN: AMSTA-TSL (Technical Library) Warren, MI 48397-5000
1	Director US Army TRADOC Analysis Command ATTN: ATAA-SL White Sands Missile Range, NM 88002-5502
(Class. only) 1	Commandant US Army Infantry School ATTN: ATSH-CD (Security Mgr.) Fort Benning, GA 31905-5660
(Unclass. only) 1	Commandant US Army Infantry School ATTN: ATSH-CD-CSO-OR Fort Benning, GA 31905-5660
1	Air Force Armament Laboratory ATTN: AFATL/DLODL Eglin AFB, FL 32542-5000
	Aberdeen Proving Ground
2	Dir, USAMSAA ATTN: AMXSY-D AMXSY-MP, H. Cohen
1	Cdr, USATECOM ATTN: AMSTE-TD
3	Cdr, CRDEC, AMCCOM ATTN: SMCCR-RSP-A SMCCR-MU SMCCR-MSI
1	Dir, VLAMO ATTN: AMSLC-VL-D

No. of Copies	Organization
2	HQDA (SARD-TR/B. Zimmerman, I. Szkrybalo) Washington DC 20310-0001
1	HQ, US Army Materiel Command ATTN: AMCICP-AD, B. Dunetz 5001 Eisenhower Avenue Alexandria, VA 22333-0001
2	Director Defense Advanced Research Projects Agency ATTN: J. Lupo J. Richardson 1400 Wilson Blvd. Arlington, VA 2209
1	Commandant US Army Armor Center ATTN: ATSB-CD-MLD Fort Knox, KY 40121
1	Commander Materials Technology Laboratory US Army Laboratory Command ATTN: SLCMT-MCM-SB, M. Levy Watertown, MA 02172-0001
1	Director US Army Laboratory Command Army Research Office ATTN: Technical Library P.O. Box 12211 Research Triangle Park, NC 27709-2211
5	Commander US Army, ARDEC ATTN: SMCAR-FSS-DA, C. Daly R. Kopmann J. Irizarry M. Oetken N. Kendl Picatinny Arsenal, NJ 07806-5000

No. of Copies	Organization
1	Commander US Army, ARDEC ATTN: SMCAR-CCS-C, T. Hung Picatinny Arsenal, NJ 07806-5000
11	Commander US Army ARDEC ATTN: SMCAR-AEE-BR, B. Brodman W. Seals A. Beardell SMCAR-AEE-B, D. Downs SMCAR-AEE-W, N. Slagg SMCAR-AEE, A. Bracuti M. Gupta J. Salo D. Chieu SMCAR-FSS-D, L. Frauen SMCAR-FSA-S, H. Liberman Picatinny Arsenal, NJ 07806-5000
4	Director Benet Weapons Laboratory US Army, ARDEC ATTN: SMCAR-CCB-DS, E. Conroy A. Graham SMCAR-CCB, L. Johnson SMCAR-CCB-S, F. Heiser Watervliet, NY 12189-4050
1	Commandant US Army Field Artillery School ATTN: ATSF-TSM-CN Fort Sill, OK 83503-5600

No. of Copies	Organization
2	Commandant US Army Field Artillery School ATTN: ATSF-CMW ATSF-TSM-CN, J. Spicer Fort Sill, OK 83503-5600
2	Commander Naval Ordnance Station ATTN: C. Dale (Code 5251) Technical Library Indian Head, MD 20640
2	Commander Naval Surface Warfare Center ATTN: O. Dengel K. Thorsted Silver Spring, MD 20902-5000
1	Commander Naval Surface Warfare Center ATTN: D.A. Wilson (Code G31) Dahlgren, VA 22448-5000
1	Commander Naval Surface Warfare Center ATTN: J. East (Code G33) Dahlgren, VA 22448-5000
1	Commander Naval Weapons Center China Lake, CA 93555-6001
1	AFOSR/NA (L. Caveny) Bldg. 410 Bolling AFB Washington, DC 20332
2	Director National Aeronautics and Space Administration ATTN: MS-603, Technical Library MS-86, Dr. Povinelli 21000 Brookpark Road Lewis Research Center Cleveland, OH 44135
1	Director Jet Propulsion Laboratory ATTN: Technical Library 4800 Oak Grove Drive Pasadena, CA 91109
3	Bell Aerospace Textron ATTN: F. Boorady F. Picirillo A.J. Friona P.O. Box One Buffalo, NY 14240
1	Calspan Corporation ATTN: Technical Library P.O. Box 400 Buffalo, NY 14225
1	General Electric Company Armament Systems Department ATTN: D. Maher Burlington, VT 05401
11	General Electric Ordnance Systems Division ATTN: J. Mandzy, OP43-220 R.E. Mayer H. West W. Pasko R. Pate I. Magoon J. Scudiere Minh Luu Lou Ann Walter Clare Cunningham R. DiNardi 100 Plastics Avenue Pittsfield, MA 01201-3698
1	IITRI ATTN: Library 10 West 35th Street Chicago, IL 60616
1	Olin Chemicals Research ATTN: David Gavin P.O. Box 586 Chesire, CT 06410-0586

No. of Copies	Organization
2	Olin Corporation ATTN: Victor A. Corso Dr. Ronald L. Dotson 24 Science Park New Haven, CT 06511
1	Safety Consulting Engineers ATTN: Mr. C. James Dahn 5240 Pearl Street Rosemont, IL 60018
2	SAIC ATTN: Dr. F.T. Phillips Dr. Fred Su 10210 Campus Point Drive San Diego, CA 92121
1	SAIC ATTN: Norman Banks 4900 Waters Edge Drive Suite 255 Raleigh, NC 27606
1	Science Applications, Inc. ATTN: R. Edelman 23146 Cumorah Crest Woodland Hills, CA 91364
1	Sundstrand Aviation Operations ATTN: Mr. Owen Briles P.O. Box 61125 Rockford, IL 61125
1	Paul Gough Associates, Inc ATTN: Dr. Paul S. Gough 1048 South Street Portsmouth, NH 03801
1	Veritay Technology, Inc. ATTN: E.B. Fisher 4845 Millersport Highway P.O. Box 305 East Amherst, NY 14051-0305
1	Director Applied Physics Laboratory The Johns Hopkins University Johns Hopkins Road Laurel, MD 20707

No. of Copies	Organization
2	Director CPIA The Johns Hopkins University ATTN: T. Christian Technical Library Johns Hopkins Road Laurel, MD 20707
1	Pennsylvania State University Department of Mechanical Engineering ATTN: Professor K. Kuo University Park, PA 16802
2	Princeton Combustion Research Laboratories, Inc. ATTN: N.A. Messina M. Summerfield 4275 US Highway One North Monmouth Junction, NJ 08852
1	University of Arkansas Department of Chemical Engineering ATTN: J. Havens 227 Engineering Building Fayetteville, AR 72701
3	University of Delaware Department of Chemistry ATTN: Mr. James Cronin Professor Thomas Bill Mr. Peter Spohn Newark, DE 19711
1	University of Illinois at Chicago ATTN: Professor Sohail Murad Department of Chemical Engineering Box 4348 Chicago, IL 60680
1	University of Maryland at College Park ATTN: Professor Franz Kasler Department of Chemistry College Park, MD 20742

No. of Copies	Organization
1	University of Michigan ATTN: Professor Gerard M. Faeth Department of Aerospace Engineering Ann Arbor, MI 48109-3796
1	University of Missouri at Columbia ATTN: Professor R. Thompson Department of Chemistry Columbia, MO 65211
1	University of Missouri at Columbia ATTN: Professor F.K. Ross Research Reactor Columbia, MO 65211
1	University of Missouri at Kansas City Department of Physics ATTN: Professor R.D. Murphy 1110 East 48th Street Kansas City, MO 64110-2499
1	University of Texas at Austin Bureau of Engineering Research ATTN: BRC EME133, Room 1.100, H. Fair 10100 Burnet Road Austin, TX 78758

No. of Copies	Organization
1	Dr. Clive Woodley GS2 Division Building R31 RARDE Ft. Halstead Sevenoaks, Kent TN14 7BT England

USER EVALUATION SHEET/CHANGE OF ADDRESS

This Laboratory undertakes a continuing effort to improve the quality of the reports it publishes. Your comments/answers to the items/questions below will aid us in our efforts.

1. BRL Report Number BRL-TR-3093 Date of Report APRIL 1990

2. Date Report Received _____

3. Does this report satisfy a need? (Comment on purpose, related project, or other area of interest for which the report will be used.) _____

4. Specifically, how is the report being used? (Information source, design data, procedure, source of ideas, etc.) _____

5. Has the information in this report led to any quantitative savings as far as man-hours or dollars saved, operating costs avoided, or efficiencies achieved, etc? If so, please elaborate. _____

6. General Comments. What do you think should be changed to improve future reports? (Indicate changes to organization, technical content, format, etc.) _____

CURRENT ADDRESS

Name

Organization

Address

City, State, Zip Code

7. If indicating a Change of Address or Address Correction, please provide the New or Correct Address in Block 6 above and the Old or Incorrect address below.

OLD ADDRESS

Name

Organization

Address

City, State, Zip Code

(Remove this sheet, fold as indicated, staple or tape closed, and mail.)

FOLD HERE

DEPARTMENT OF THE ARMY
Director
U.S. Army Ballistic Research Laboratory
ATTN: SLCBR-DD-T
Aberdeen Proving Ground, MD 21005-5066
OFFICIAL BUSINESS

NO POSTAGE
NECESSARY
IF MAILED
IN THE
UNITED STATES

BUSINESS REPLY MAIL
FIRST CLASS PERMIT No 0001, APG, MD

POSTAGE WILL BE PAID BY ADDRESSEE

Director
U.S. Army Ballistic Research Laboratory
ATTN: SLCBR-DD-T
Aberdeen Proving Ground, MD 21005-9989

FOLD HERE